HOMO−LUMO Gap as an Index of Molecular Size and Structure for Polycyclic Aromatic Hydrocarbons (PAHs) and Asphaltenes: A Theoretical Study. I

Yosadara Ruiz-Morales*

Programa de Ingeniería Molecular, Instituto Mexicano del Petróleo, Eje Lázaro Cárdenas 152, Mexico City 07730, Mexico

Received: May 8, 2002; In Final Form: August 6, 2002

Theoretical calculations are presented for the effect on the HOMO−LUMO gap due to the successive addition of aromatic rings and their different distributions, isomers, for polycyclic aromatic hydrocarbons (PAHs). The study is based on ZINDO/S calculations. PAHs with 1−14 fused aromatic rings (FAR) are considered. The results of these calculations are addressed to a currently existing controversy regarding the number of FAR in asphaltene structures. Asphaltenes are considered as polycyclic aromatic compounds similar to PAHs but containing heteroatoms and alkyl side chains. The theoretical results are compared with fluorescence emission (FE) experimental data. It is found that the asphaltene experimental FE range does not necessarily correspond to different chromophores with different number of FAR but may be different isomers with the same number of FAR. Also, the effect of the presence of alkyl chains and heteroatoms in the asphaltene structures on the HOMO−LUMO gap is almost negligible. We conclude that the FAR region in asphaltenes has PAH chromophores with 5−10 fused rings. The 100% compactness (circular) PAH structures, beyond 10 fused rings, and the 0% compactness (linear or zigzag) PAH structures are not possible for asphaltenes. Relationships between the HOMO−LUMO gap and structural parameters for PAH chromophores in asphaltenes were found. The effect of the number of FAR and Clar sextets, the compactness, and longest dimension on the HOMO−LUMO gap of PAHs is evaluated.

1. Introduction

Petroleum asphaltenes are the heaviest, most aromatic, and most polar fractions of heavy oils and bitumen. Asphaltenes are considered to be the most problematic components in oil recovery, transportation, and refinery upgrading. Asphaltenes are often present in colloidal forms dispersed in the surrounding oil matrix. However, as a result of slight changes in conditions during oil production, transportation, and refining, the asphaltenes colloidal disperse phase separates, forming very stable solid asphaltene aggregates. In catalytic processes, asphaltenes cause severe catalyst deactivaton.[1−6]

The presence of asphaltenes has a negative impact on both the physical and chemical properties of heavy oils and increases the difficulties of crude oil utilization by impacting the processability of these heavy hydrocarbons.

Asphaltenes are defined in terms of a solubility classification, not by chemical structure, because of the difficulty of defining experimentally their structure. A widely used definition of petroleum asphaltenes is that they are the petroleum component that is insoluble in *n*-heptane and soluble in toluene.[1−6]

Asphaltenes are among the least understood deposits occurring in the oil field, and in most cases, the structure of the asphaltenes is not known. They are thought to be polycyclic aromatic compounds (PACs) similar to polycyclic aromatic hydrocarbons (PAHs) but containing heteroatoms (N, O, S) and alkyl side chains in their structure.

There have been a number of experimental studies of asphaltenes. Early investigations of the molecular structure of asphaltenes have suggested that they consist of large condensed aromatic systems with 10 fused rings in each aromatic system connected by alkyl or sulfur linkages.[7−9] The average asphaltene molecule was thought to contain 40−70 condensed aromatic systems. Recent studies, however, have suggested that the asphaltene molecules are significantly smaller with an average polyaromatic core size of 5−7 aromatic systems with 10 fused rings each connected by alkyl or sulfur linkages.[10−12]

Fluorescence depolarization techniques have been used to correlate the molecular size of asphaltenes with the constituent chromophore size. This work suggests that asphaltenes present a polyaromatic core size of 1−2 aromatic systems with 4−10 fused rings in each one.[6,13−14] It was also concluded that the range of asphaltene molecular diameters is 10−20 Å and they have a molecular mass of 500−1000 amu. The experimental asphaltene fluorescence emission is significant in the range of 400−650 nm. Thus, the range of the number of fused rings in an individual aromatic system in asphaltenes can be determined by fluorescence emission studies.[13] However, it is difficult to use the fluorescence emission spectrum to obtain an exact distribution of the fused rings and sizes because the optical absorption and emission constants are different for different chromophores.

Despite all of the investigations of the molecular structure of asphaltenes, there are large disagreements in the reached conclusions. Because of the uncertainty in the number of aromatic systems—or also known as fused aromatic rings—in asphaltenes and the uncertainty in the number of fused rings in each aromatic system, there is a controversy regarding the molecular weight[15] of asphaltenes. The most recent values published are 10 000,[16] 800,[17,18] 400,[10] >6000,[19] and 500−1000 amu.[13] Mass spectroscopy results were used to measure the number of

* E-mail: yruiz@imp.mx.

10.1021/jp021152e CCC: $22.00
Published on Web 10/29/2002

aromatic rings per molecule, but these results are unable to distinguished bonded from separated aromatic systems.[10]

Regarding the number of fused rings in each aromatic system in asphaltenes, there are reports that range from 4 to 20 fused rings.[1−6,13] However, the larger number of fused rings is incompatible with low molecular weights. Several experimental techniques suggest that the average value of fused rings in the aromatic systems is <10.[13] Scanning tunneling microscopy (STM) has been used to image the aromatic systems in asphaltene molecules. The size obtained of the fused aromatic systems is about 10 Å.[20]

However, the broad classes of experimental studies do not tell us what the structures of the asphaltene molecules actually are. To understand the phenomenon of aggregation of asphaltenes and their interactions with metals and resins, it is important to know their chemical and electronic structures. This information will allow us to design separation systems, to design catalysts for their decomposition, as well as to avoid their deposition, and to characterize the heavy fraction of crude oil. The goal is to predict the structures of asphaltenes. Such an understanding is important if we are to get the optimal use from the heavy fraction of any crude oil.

Computational chemistry approaches have revolutionized our understanding of the structure and reactivity of molecules. In the present study, we use theoretical chemistry to address the controversy regarding the number and size of fused rings and their possible distributions in the individual aromatic systems in asphaltenes.

In this study, we carried out theoretical calculations for the effect on the HOMO−LUMO gap due to the successive addition of aromatic fused rings and their different distributions (isomers) for polycyclic aromatic hydrocarbons (PAHs). As stated above, asphaltenes are considered as polycyclic aromatic compounds (PACs) similar to PAHs but containing heteroatoms and alkyl side chains in their structure. Systems with 1−14 fused aromatic rings are considered explicitly. The theoretical results are compared with the experimental results obtained from fluorescence emission data for asphaltenes to conclude about the structural features and the total number of the fused rings in asphaltenes that produce the observed fluorescence emission. These results were used to validate some asphaltene structures reported in the literature.

It can be considered, as we show in this study, that the stability and reactivity of asphaltene molecules is closely associated with the stability and reactivity of their polycyclic aromatic hydrocarbon core. In this paper, we systematically analyze the relationship between the structure of PAH isomers and the number of resonant sextets present. The number of resonant sextets in the structure is closely related to the HOMO−LUMO gap magnitude.

The HOMO−LUMO gap is used as a direct indicator of kinetic stability.[21−28] A large HOMO−LUMO gap implies high kinetic stability and low chemical reactivity because it is energetically unfavorable to add electrons to a high-lying LUMO or to extract electrons from a low-lying HOMO.[21−23]

Clar[29,30] observed that the more highly colored a PAH (high wavelengths in the visible spectrum) is, the less stable it is, kinetically. Thus, he related kinetic instability to a small HOMO−LUMO gap. It has been showed that for benzenoid PAHs there is a correlation between the HOMO−LUMO gap and the Hess−Schaad resonance energy per π electron, which is a measure of thermodynamic stability due to cyclic conjugation.[31−33] This correlation indicates that, in general, thermodynamically stable PAHs are kinetically stable.

A Clar structure[29,30] for a PAH molecule is depicted as a combination of the maximum number of isolated and *localized* aromatic sextets for that molecule with a minimum number of localized double bonds.[31] In general, a PAH molecule with a given number of aromatic sextets is kinetically more stable than its isomers with fewer aromatic sextets.[29]

Each isomer of a PAH within a family, with the same number of fused rings, presents a certain number of Kekulé resonance structures. Each Kekulé structure has a different number of resonant rings. Only the Kekulé resonance structures with the maximum number of aromatic sextets have the lowest energy. It has been proven that the resonance interactions in these sextets have the largest contribution to the resonance energy,[34] in line with Clar's model.[29,30] The term "aromatic stabilization"[35−40] is still well-accepted and is estimated to be 36 kcal/mol for benzene, that is, for each resonant sextet present in the PAH structure.

Besides the Hückel rule, which strictly applies to monocyclic polyene, several attempts to characterize the aromaticity solely from structural information have been presented in the literature, such as the scheme of Platt,[41] the scheme of Volpin,[42] and the scheme of Craig.[43] The scheme of Platt employs π-electron periphery and makes an emphasis on the number of electrons. The scheme of Platt fails in many instances in the interpretation of the aromatic behavior of PAHs. The scheme of Volpin attempts to characterize cata-condensed fused rings, again using the number of π electrons as a critical factor. The scheme of Craig considers symmetry properties of molecular orbitals and valence bond approximated descriptions of conjugated π systems. These schemes in many instances provide a useful indication of the aromatic nature of a molecule; however, in many instances they are in apparent contradiction with chemical evidence.

Hosoya[44] et al. and Aihara[45] proposed the extension of the Hückel rule, which can reasonably be applied to the PAH systems. Hosoya et al.[44] introduced a modified semianalytical topological index as stability criterion of PAHs. The modified topological index is proposed for estimating the total π-electron energy. They found that individual benzene rings are the main contributors to the aromaticity of polycyclic molecules in agreement with Clar's model.[29] Other approaches in the literature to aromaticity criteria are the Herndon−Randic theory of conjugated circuits, Aihara's graph-theoretical theory,[46] and Schleyer's nuclear independent chemical shift (NICS) values.[47] All of these theories are consistent with the Clar concept of aromatic sextets.[29,30]

Several aromaticity indices are defined in the literature on the basis of different criteria.[36] There are energy-, geometry-, and magnetic-based aromaticity indices. The magnetic-based aromaticity indices such as NICS[47] are related to the magnetic properties of molecules. The energy-based aromaticity indices are grounded on energetic criteria.[35] These indices are based on the calculation of the resonance energy and stabilization. The geometry aromaticity indices are based on bond lengths.[36] These indices have the disadvantage that they overestimate the aromatic character when the molecule has all bonds of equal length. The geometry-based descriptors of aromaticity may not always be in line with other descriptors.[36] On the other hand, the topological characteristics of a molecule affect its aromaticity. The aromaticity in PAH for individual rings changes depending dramatically on the topological position of the ring.[36]

All of the above theories are pointing toward the existence of localized cyclic resonant sextets in PAH systems. Polycyclic aromatic hydrocarbon isomers have the same number of fused

rings and same number of π electrons. However, the PAH isomers may have or may not have the same number of localized resonant sextets in their structure although they have the same number of π electrons. Thus the structural isomers with the highest number of resonant sextets in their structure will have a higher stability than the structural isomers with a smaller number of resonant sextets.

None of the aromaticity theories presented above provides, in an easy way, information about the maximum number of resonant sextets present in PAH structural isomers and their topological localization in the structure. To understand the observed 0-0 band fluorescence emission of asphaltenes and PAH, as well as their stability and reactivity, it is important to know about the number of the resonant sextets and their localization in the structures.

In this paper, we present a new qualitative rule that we have called *Y-rule* that helps to determine the number of resonant sextets and to draw their most likely localization in homologous series of polycyclic aromatic hydrocarbon compounds and in the fused ring region in asphaltenes. The Y-rule only applies for the peri-section of the fused ring region in asphaltenes and in PAH with fused six-member rings. This rule allows us to determine the positions of the resonant sextets without having to calculate the electronic structure of the system and thus to determine the maximum number of sextets in the FAR region.

PAH compounds possess topological characteristics that are common between isomers having the same molecular formula. Dias[48−53] has broadly studied these topological characteristics and proposed a periodic table for benzenoid PAHs. However, as pointed out by Acree,[54] the Dias periodic table does not distinguish between the different PAH isomers. The qualitative Y-rule helps in locating the resonant sextets in each PAH isomer.

Our Y-rule is based on topological information of the PAH system, such as the number of π electrons and number of fused rings, and on molecular connectivity and quantities derived from such information, and to the best of our knowledge, the Y-rule is the first of its kind. We could not find in the literature another rule similar to Y-rule. The topological characteristics of benzenoid PAHs are extrapolated to the aromatic fused regions in asphaltenes.

2. Computational Details

In the present theoretical study, we have only concentrated in studying the neutral even-numbered PAHs with fused six-member rings, that is, benzenoid-type PAHs. The asphaltene models were taken from the literature. Only petroleum asphaltenes are studied. Theoretical calculations are presented for the effect on the HOMO−LUMO gap due to the successive addition of aromatic rings and their different distributions (isomers) for polycyclic aromatic hydrocarbons (PAHs). Systems with 1−14 fused aromatic rings (FAR) are considered. A total of 95 PAHs were studied. Only the most representative results are presented. The theoretical HOMO−LUMO transitions are compared with experimental fluorescence emission corresponding to the 0-0 band of the fluorescence spectrum of free PAHs and of petroleum asphaltenes. The results of the general tendencies in PAHs are extrapolated to asphaltenes.

The structure optimization of the PAH systems and the asphaltenes was done by performing force field-based minimization using the energy minimization panel in Cerius2, version 4, and the COMPASS consistent force field as it is provided in the Cerius2 package.[55]

COMPASS (condensed-phase optimized molecular potentials for atomistic simulation studies) force field was used in all of the optimizations because it has been tested and validated extensively against experiment for many organic molecules. It is an ab initio force field that enables accurate and simultaneous prediction of gas-phase properties (structural, conformational, vibrational, etc.) and condensed-phase properties (equation of state, cohesive energies, etc.) for a broad range of molecules and polymers.[56,57]

In a previous study,[58] to be published elsewhere, we carried out the validation of the best combination of theoretical methods (optimization method//excited states calculation method and optimization method//single-point calculation method) that agree better with the experimental fluorescence emission data of PAHs. With this in mind, the excited states (including the HOMO−LUMO transition) of 95 well-known PAH compounds were studied. The optimization of structures was carried out using COMPASS force field-based minimization (FF) and the semiempirical PM3 method. Excited states were calculated with the ZINDO/S, CIS, and DFT-TD methods. The ZINDO/S calculations using the FF-optimized structures gave excited states in better agreement with experiment. Then, several combinations of theoretical methods to calculate the most reliable MO energies, that is, those that reproduce the HOMO−LUMO gap obtained with ZINDO/S, were tested (optimization method//single-point calculation method) B3LYP//B3LYP, HF, BLYP, PM3 and PM3//B3LYP, HF, BLYP, PM3 and FF//B3LYP, HF, BLYP. It was found that the FF//B3LYP combination with a 6-311G(d,p) basis set is the best combination that reproduces the HOMO−LUMO gaps obtained from the ZINDO/S calculations and gives the most reliable MO energies.

Thus, in the present study, the excited electronic states (including the HOMO−LUMO configuration) of the PAH compounds and the asphaltenes were calculated using ZINDO/S[59] as it is provided in the Gaussian 98 package,[60] employing the COMPASS force field (FF)-optimized structures.

3. Results and Discussion

We shall now provide a discussion of how the HOMO−LUMO gap is modified because of the successive addition of aromatic fused rings and their different distributions (isomers) in polycyclic aromatic hydrocarbons (PAHs) and to interpolate the main conclusions to the fused rings region of an individual aromatic system in asphaltenes. The discussion will start with free PAHs and continue to asphaltenes in the next sections.

In the present theoretical study, we have only concentrated in studying the neutral even-numbered PAHs with fused six-member rings, that is, benzenoid-type PAHs. The asphaltene models were taken from the literature, and they also present an aromatic system that is formed with benzenoid-fused rings. From the ZINDO/S results, the HOMO−LUMO transition has been identified in terms of the dominant singly excited configurations.

The theoretical HOMO−LUMO transitions are compared with experimental fluorescence emission corresponding to the 0-0 band of the fluorescence spectrum. It is important to remember that the fluorescence emission spectrum shows emission predominantly from the single lowest vibrational state in the lowest excited electronic state to a series of vibrational states (0, 1, 2, 3, etc.) of the ground electronic state. In the 0-0 band notation, the first number corresponds to the lowest vibrational state of the excited electronic state and the second number corresponds to the lowest vibrational state of the ground electronic state. The energy gap between the ground and first exited state (within a given spin manifold) corresponds to the HOMO−LUMO gap. Thus, the λ_{0-0} corresponds to the wavelength associated with a transition that is related to the

TABLE 1: Table with Abbreviations and Definitions of Terms Employed within the Text and in Other Tables

abbreviation	definition
PAH(s)	polycyclic aromatic hydrocarbon(s)
FAR	fused aromatic ring
nFAR	number of total fused aromatic rings (both localized resonant rings and those with no resonance); nFAR = $(C_{Int} + 2)/2$
FRS or TRS	full resonant structure, previously defined as TRS (total resonant structure) by Dias.[48−53]
N_R	number of localized resonant rings in the FAR region, three double bonds that in total involve six π-electrons and that are permutable within the same hexagonal ring, that is, number of aromatic sextets in the structure. For calculation, see eqs 10−13 in the text
C_A	total carbons in the FAR region (both aromatic carbons that are part of localized resonant rings and aromatic carbons that are part of localized double bonds)
H_A	peripheral protonated carbons in the FAR region or the total number of hydrogen atoms present if the FAR region were completely unsubstituted as in PAH compounds
C_{Ar}	total number of aromatic carbons in localized resonant rings or total number of carbon atoms involved in resonant sextets; $C_{Ar} = 6(N_R)$
H_{Ar}	aromatic protonated carbons or total hydrogen atoms bonded to carbon atoms in localized resonant rings (i.e., in aromatic sextets); $H_{Ar} = C_{Ar} - C_{PAr3} - C_Y$
C_{DB}	total number of carbons in localized double bonds in the FAR region; $C_{DB} = C_A - C_{Ar}$
N_{DB}	total number of localized double bonds in the FAR region; $N_{DB} = C_{DB}/2$
C_{Int}	total internal bridging carbons in the whole FAR region (in localized resonant rings or localized double bonds); $C_{Int} = C_A - H_A = C_Y + C_{PA3} = 2(\text{nFAR}) - 2$ (previously defined by Dias[48−53])
C_{IntAr}	total internal bridging carbons in the FAR region only in localized resonant rings; $C_{IntAr} = C_Y + C_{PAr3}$
d_s	net number of disconnections among the internal edges in the FAR region; $d_s = C_{PA3} - \text{nFAR}$; term defined by Dias[48−53]
C_Y	number of Y-carbons, internal aromatic carbons in the whole FAR region having a connectivity of 3 (Figure 5); $C_Y = -2 + \text{nFAR} - d_s$. For cata-condensed systems, $C_Y = 0$. This term was originally defined by Dias as N_{Ic}[48−53]
C_{PA3}	peripheral aromatic carbons in the whole FAR region having a connectivity of 3; $C_{PA3} = C_{Int} - C_Y = \text{nFAR} + d_s$. For cata-condensed systems, $C_{PA3} = C_{Int}$ (Figure 5). This term was originally defined by Dias as N_{Pc}[48−53]
C_{PAr3}	peripheral aromatic carbons in localized resonant rings in the FAR region having a connectivity of 3; $C_{PAr3} = C_{PA3} - I_{even}$, $I = 2, 4, 6, ...$, until $C_{PAr3} = 4$ or $C_{PAr3} = C_{IntAr} - C_Y = C_{Ar} - H_{Ar} - C_Y$. For cata-condensed systems, $C_{PAr3} = C_{IntAr}$
P_C	percentage of compactness. It is a measure of the degree of condensation of the PAH structure. The lowest value of P_C is 0%, and the highest value is 100%

HOMO−LUMO gap. For organic molecules without heavy atoms, spin−orbit coupling is generally weak, yielding allowed optical transitions only within a given spin manifold.[61,62] Therefore, in general for the study here presented, it is a good approximation to consider the 0-0 band of the fluorescence spectrum as a direct measurement of the HOMO−LUMO gap.

To simplify the notation for the orbitals, the occupied MOs in the ground-state configuration will be denoted as H, H − 1, H − 2, etc. for HOMO, HOMO − 1, HOMO − 2, etc., correspondingly. The unoccupied MOs will be denoted L, L + 1, L + 2, ... for LUMO, LUMO + 1, LUMO + 2, ..., respectively.

4. Structure of Free Polycyclic Aromatic Hydrocarbon Compounds (PAHs)

Throughout this section, we will be using many terms and abbreviations. All of the terms and abbreviations used are gathered and defined in Table 1. We will discuss each term along the text. Dias[48−53] has previously defined some of the terminology in Table 1. Some of the symbols have been changed to avoid confusions. For definitions in this section, refer to Table 1 when needed.

In the present theoretical study, we have only concentrated in studying the neutral even-numbered PAHs with fused six-member rings, that is, benzenoid-type PAHs. Benzenoid PAHs contain an even number of carbon atoms. In general, benzenoid PAHs are restricted to a range of stoichiometries. Thus, to decide about the particular type of PAH molecules to calculate, we had to find all of the possible stoichiometries that define the benzenoid PAHs and their molecular structures.

The number of fused rings, benzenoid-type, or the number of fused aromatic rings (nFAR), is related to the stoichiometry of the PAHs. The carbon (C_A) and hydrogen (H_A) content of each PAH has a direct relationship with nFAR found by Dias[48−53] and presented in eqs 1 and 2.

$$\text{nFAR} = \frac{(C_{Int} + 2)}{2} \tag{1}$$

$$C_{Int} = C_A - H_A \tag{2}$$

C_{Int} is related to the total internal bridging carbons in the whole fused aromatic ring (FAR) region in PAHs. The subindex A in C_A and H_A stands here for aromatic. The fused ring regions in asphaltenes have been concluded to be aromatic by NMR.[1−3,5,63] Thus, the abbreviations used in this section will be useful also in the following sections for asphaltenes.

In Figure 1, the PAH stoichiometries are presented in a nFAR vs hydrogen content diagram. An important amount of information can be withdrawn from this diagram. Figure 1 is a schematic adaptation of the Dias periodic table for benzenoid PAH.[48] As it can be seen in Figure 1, all of the benzenoid PAH stoichiometries are restricted to a region delimited by two border lines. Any other stoichiometries outside the border lines do not correspond to benzenoid PAHs.

The systems on the lower-limit curve, represented by squares, are pure cata-condensed with the least compact structure, such as the linear or zigzag structures. In Figure 2, there are some examples of cata-condensed systems.

The systems on the upper-limit curve, represented by circles, are pure peri-condensed systems with the most compact (circular) structure. In Figure 3, the pure peri-condensed PAHs are presented (marked with an asterisk) together with the most compact systems of each nFAR series. There is only one

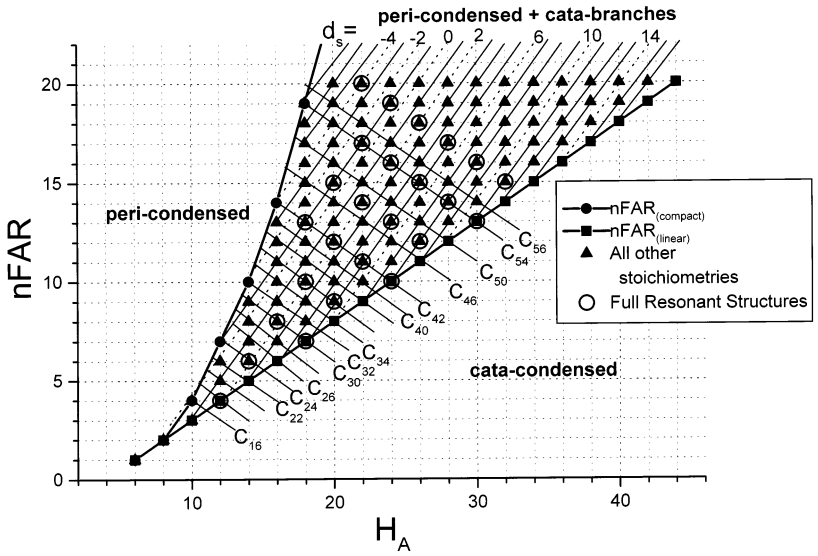

Figure 1. Diagram of the number of fused aromatic rings (nFAR) versus hydrogen content (H_A) for benzenoid polyaromatic hydrocarbon compounds (PAHs). The stoichiometries of all of the PAHs up to 20 fused aromatic rings (FARs) are presented. The equations for the upper limit curve, which contains the pure peri-condensed circular compounds, and the lower limit curve, which contains the cata-condensed compounds, are given in Table 2. In the diagram, there are lines that mark all of the stoichiometries with the same number of carbon atoms. Lines that mark all of the stoichiometries with the same net number of disconnections among the internal edges (d_s) in the structure are also shown.

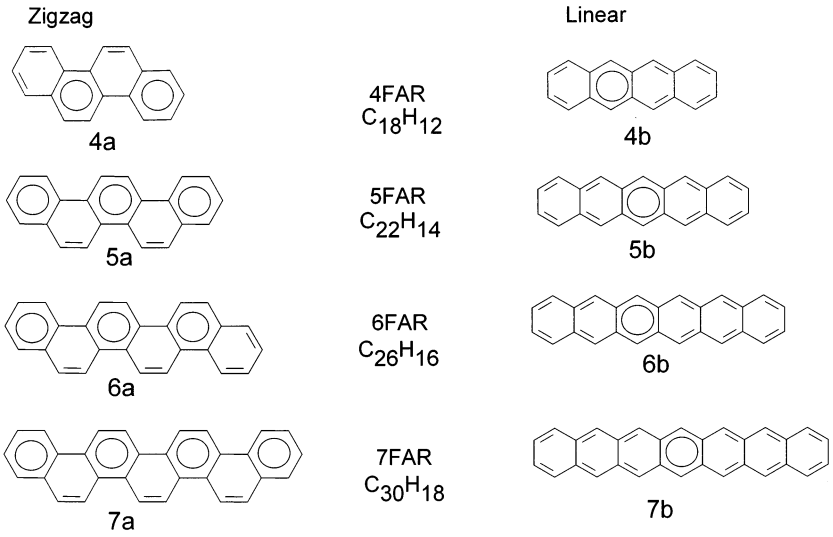

Figure 2. Structures of linear and zigzag compounds for PAH systems with four to seven fused aromatic rings. The stoichiometries of these systems are given by the lower limit curve in Figure 1 and in Table 3.

isomer for those stoichiometries nearest to or on the upper-limit curve. The compact, circular benzenoids are the D_{6h} polycircumcoronene and matching D_{2h} polycircumovalene and polycircumpyrene, constant-one-isomer series discovered by Dias.[48−53] All of the other stoichiometries, represented by triangles in Figure 1, which lie between the two border lines, represent systems that have a peri-condensed core with cata-branches.

The equations that define the upper and lower border lines are given in Table 2. Also, equations to determine the C_A and H_A content for systems on the curves are given. We found that the best equation that describes the upper border curve is eq 3.

$$C_A = -\frac{1}{3} + \frac{{H_A}^2}{6} \qquad (3)$$

Siegmann[64] and co-workers had previously come to conclusions about the existence of the border line curves for the benzenoid PAH stoichiometries. The equation that they found for the upper limit was $C_A = {H_A}^2/6$. In both cases, the systems on the pure peri-curve were obtained by the concept of arranging circles of hexagons around the benzene core and pyrene core. This concept is part of the enumeration algorithm developed by Dias.[48−53]

For each nFAR or each nFAR row, there are a given number of possible stoichiometries. For example, for six aromatic fused rings (6FAR), there are three possible stoichiometries: $C_{22}H_{12}$, $C_{24}H_{14}$, and $C_{26}H_{16}$.

All of the systems crossed by a line depicting the carbon content have exactly the same carbon content, but what is different is the hydrogen content. On the other hand, it can be seen from Figure 1 that there are many stoichiometries that present the same hydrogen content but different carbon content. Within one sequence, the number of hydrogen atoms is the same, while the number of carbon atoms increases by 2. In Table 3, all of the stoichiometries for benzenoid PAHs from 2FAR to 10FAR are given together with the percentage of compactness (P_C) as we define it here.

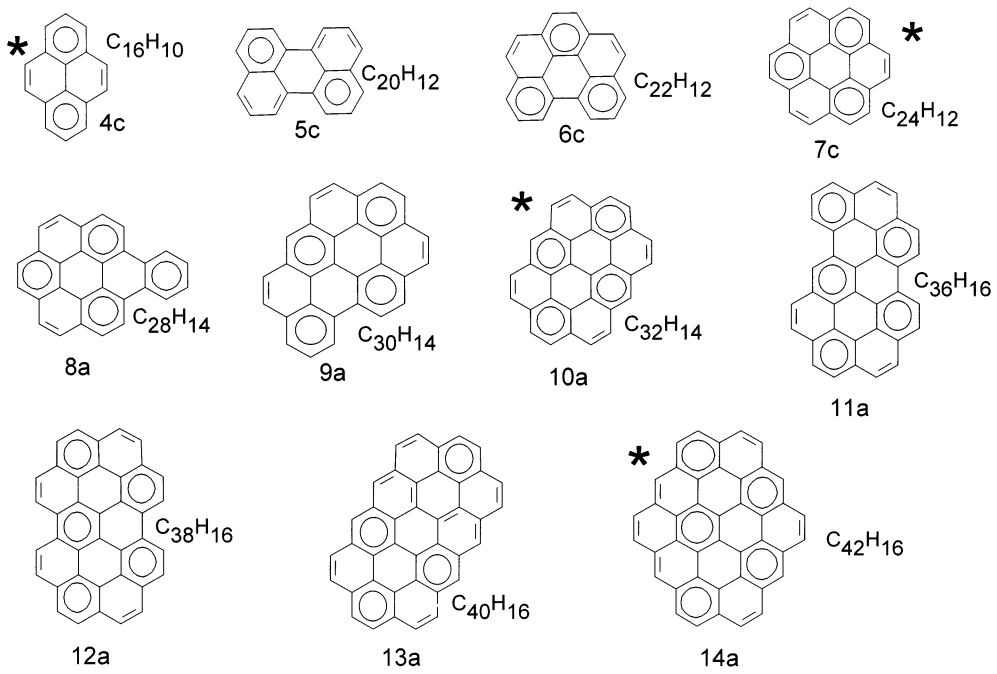

Figure 3. Structures of compact compounds for PAH systems with 4 to 14 fused aromatic rings. The stoichiometries of the systems that are totally circular or with 100% of compactness are given by the upper limit curve in Figure 1 and in Table 3. These systems are 4FAR (pyrene), 7FAR (coronene), 10FAR (ovalene), and 14FAR (circumpyrene), and they are marked with an asterisk. The rest of the structures in the figure have the highest percentage of compactness that can be reached for that given number of FARs. There is only one isomer for those stoichiometries nearest to or on the upper limit curve in Figure 1.

TABLE 2: Borderline Curves for PAH Systems[a]

Cata-Condensed PAHs (Lower Limit)
$C_A = -6 + 2H_A$
$H_A = (C_A + 6)/2$
nFAR $= (C_A - 2)/4$ or nFAR $= (H_A/2) - 2$
$C_{Int} = C_A - H_A = -2 + 2$nFAR
Compact Circular PAHs (Upper Limit)
$C_A = (-1/3) + (H_A^2/6)$
$H_A = \sqrt{6C_A + 2}$
nFAR $= 0.8333 + (H_A^2/12) - (H_A/2)$ or nFAR $= 1.0833 + (C_A/2) - (\sqrt{6C_A + 3})/2$
$C_{Int} = C_A - H_A = -2 + 2$nFAR

[a] For definitions of abbreviations, see Table 1.

The percentage of compactness (P_C) is a measure of the degree of condensation of the PAH structure. The lowest value of P_C is 0%, and the highest value is 100%. The PAHs with 0% of compactness have a structure that is the least compact; this is the case for cata-compounds. The PAHs with 100% of compactness have a structure that is the most compact; this is the case for the pure peri-condensed (circular) systems. The percentage of compactness for all of the stoichiometries between the border lines is calculated by interpolation.

It is observed from Figure 1 that for the same carbon content as the hydrogen content becomes higher, the percentage of compactness becomes lower. The systems on the lower border line (0% P_C) have more hydrogen content than the systems on the upper border (100% P_C). Thus, the hydrogen content gives the percentage of condensation. For a given carbon content, the hydrogen content calculated with the formula of the upper curve (eq 4) corresponds to a stoichiometry with 100% of compactness. The hydrogen content calculated with the lower limit curve (eq 5) corresponds to a stoichiometry with 0% of compactness. A linear extrapolation of these points in a diagram P_C vs hydrogen content for the same carbon content provides an equation with which the P_C of other stoichiometries with the same carbon content can be calculated.

$$H_A = \sqrt{6C_A + 2} \tag{4}$$

$$H_A = \frac{C_A + 6}{2} \tag{5}$$

In Table 3, the benzenoid PAH stoichiometries for 2FAR to 10FAR are presented. Stoichiometries beyond 10FAR can be deduced from Figure 1. The percentage of condensation (P_C) for all of the stoichiometries is also presented in Table 3. In a FAR series, the highest stoichiometry corresponds to the lowest P_C and the lowest stoichiometry corresponds to the highest P_C.

4.1. Topological Characteristics of Polyaromatic Hydrocarbons. The HOMO−LUMO gap of PAHs depends on the size in terms of the number of fused rings (nFAR) but also upon the nature of the periphery.[65−69] Dias[50,51] showed that there are four types of CH perimeter units on the outer boundary of PAHs, Figure 4: the bay regions (no CH) designated by η_0, solo units (one CH) designated by η_1, duo units (two proximate CHs) designated by η_2, trio units (three proximates CHs) designated by η_3, and quarto units (four proximate CHs) designated by η_4. The perimeter topology of peri-PAHs follows the eq 6. The number of solo (η_1) groups is independent of eq 6. Dias[50] concluded that magic-angle NMR of benzenoid solids composed of constituents of peri-condensed benzenoids should yield considerable information by determining the ratio of η_1 to η_2.

$$-\eta_0 + \eta_2 + 2\eta_3 + 3\eta_4 = 6 \tag{6}$$

Proximate doublets and triplets of bay regions define the coves and fjords, respectively (Figure 4), that are also present in some PAHs.[51]

The topological elements that are common to all PAH isomers having a given benzenoid molecular formula include the following:[48−53] (a) the number of σ-bonds; (b) the number of

TABLE 3: Number of Nonradical Isomers Associated with Each Stoichiometry of FAR Systems and Structural Parameters

system	stoichiometry[f]	P_C[d], %	number of isomers[a]	N_R[b]	N_{DB}	d_s	C_Y	C_{PA3}	C_{Int}
2FAR	$C_{10}H_8$	0	1	1	2	0	0	2	2
3FAR	$C_{14}H_{10}$	0	2	2, 1	1, 4	1	0	4	4
4FAR	$C_{16}H_{10}$	100	1[i]	2	2	0	2	4	6
	$C_{18}H_{12}$	0	5 (1)[e]	3 (full),[g] 2, 1	0, 3, 6	2	0	6	6
5FAR	$C_{20}H_{12}$	50	3	3, 2	1, 4	1	2	6	8
	$C_{22}H_{14}$	0	12	3, 2, 1	2, 5, 8	3	0	8	8
6FAR	$C_{22}H_{12}$	82	2	3, 2	2, 5	0	4	6	10
	$C_{24}H_{14}$	33	13 (1)[e]	4 (full),[g] 3, 2	0, 3, 6	2	2	8	10
	$C_{26}H_{16}$	0	37	4, 3, 2, 1	1, 4, 7, 10	4	0	10	10
7FAR	$C_{24}H_{12}$	100	1[i]	3[h]	3	−1	6	6	12
	$C_{26}H_{14}$	65	9	4, 3, 2	2, 4, 7	1	4	8	12
	$C_{28}H_{16}$	25	62	4, 3, 2	2, 5, 8	3	2	10	12
	$C_{30}H_{18}$	0	123[c](1)[e]	5 (full),[g] 4, 3, 2, 1	0, 3, 6, 9, 12	5	0	12	12
8FAR	$C_{28}H_{14}$	75	8	4, 3, 2	2, 5, 8	0	6	8	14
	$C_{30}H_{16}$	45	58 (1)[e]	6 (full),[g] 5, 4, 3, 2	0, 3, 6, 9, 12	2	4	10	14
	$C_{32}H_{18}$	20	295[c]	5, 4, 3, 2	1, 4, 7, 10	4	2	12	14
	$C_{34}H_{20}$	0	446[c]	5, 4, 3, 2, 1	2, 5, 8, 11, 14	6	0	14	14
9FAR	$C_{30}H_{14}$	89	3	4,[h] 3, 2	3, 6, 9	−1	8	8	16
	$C_{32}H_{16}$	60	46	5, 4, 3, 2	1, 4, 7, 10	1	6	10	16
	$C_{34}H_{18}$	33	335[c]	5, 4, 3, 2	2, 5, 8, 11	3	4	12	16
	$C_{36}H_{20}$	16	1440[c] (1)[e]	6 (full),[g] 5, 4, 3, 2	0, 3, 6, 9, 12	5	2	14	16
	$C_{38}H_{22}$	0	1689[c]	6, 5, 4, 3, 2	1, 4, 7, 10, 13	7	0	16	16
10FAR	$C_{32}H_{14}$	100	1[i]	4	4	−2	10	8	18
	$C_{34}H_{16}$	66	34	5, 4, 3, 2	2, 5, 8, 11	0	8	10	18
	$C_{36}H_{18}$	49	337 (3)[e,]	6 (full),[g] 5, 4, 3, 2	0, 3, 6, 9, 11	2	6	12	18
	$C_{38}H_{20}$	28	1987[c]	6, 5, 4, 3, 2	1, 4, 7, 10, 13	4	4	14	18
	$C_{40}H_{22}$	14	6973[c]	6, 5, 4, 3, 2	2, 5, 8, 11, 14	6	2	16	18
	$C_{42}H_{24}$	0	6693[c] (1)[e]	7 (full),[g] 6, 5, 4, 3, 2, 1	0, 3, 6, 9, 12, 15, 18	8	0	18	18

[a] References 48 and 50. [b] Equations 10−13 (see text). [c] Does not includes stereoisomers. [d] Percentage of compactness. Absolute peri-systems, also known as circular systems, have $P_C = 100\%$; these are the most compact PAHs. The absolute cata- or kata-systems have $P_C = 0\%$, these are the least compact systems. For cata-systems, C_Y is always zero (see text). [e] Number of isomers with full resonant sextet structures and no localized double bonds. From 4FAR to 9FAR, there is only one full resonant structure. From 10FAR to 20FAR, there are more than one full resonant isomer for a given stoichiometry, but those systems with P_C near to 70%−79% have only one full resonant structure. [f] The number of π-electrons is equal to the total number of carbons, that is, π-electrons $= C_A$. [g] Total number of resonant sextets in the full resonant sextet structure. [h] Although the total number of π-electrons in each of these stoichiometries is divisible by six, they cannot be full resonant structures or reach the highest N_R because their P_C is higher than 79% from 7FAR on. [i] The systems with 100% of compactness, that is, those systems on the upper limit (Figure 1), have only one isomer.

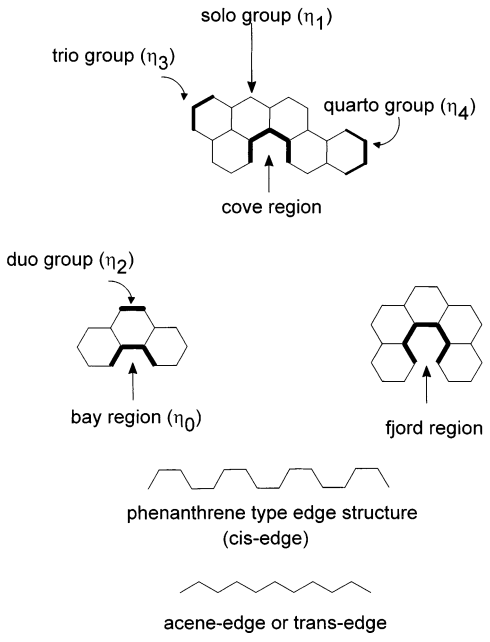

Figure 4. Schematic representation of the structural parameters in polyaromatic hydrocarbon compounds and the different type of edges in the PAH structure.

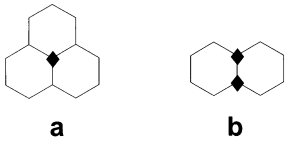

Figure 5. Schematic representations of (a) internal aromatic Y-carbons in the FAR region with a connectivity of three and (b) peripheral aromatic carbons in the whole FAR region with a connectivity of three.

fused aromatic rings (nFAR); (c) the carbon and hydrogen content (C_A and H_A, respectively); (d) the number of internal aromatic carbons with a connectivity of 3 (C_Y); (e) the number of peripheral aromatic carbons having a connectivity of 3 (C_{PA3}); (f) the total internal bridging carbons, C_{Int}; (g) the net number of disconnections among the internal edges, d_s. Many of the mentioned terms are related by mathematical expressions, which are given in Table 1. The number of internal aromatic carbons with a connectivity of 3, C_Y, is equal to the number of carbons in third-degree vertexes, bounded by three hexagonal rings (Figure 5). We denominate these carbons as internal Y-carbons (C_Y) because they are in the center of what looks like a Y letter. The number of peripheral aromatic carbons having a connectivity of 3, C_{PA3}, is equal to the number of carbon atoms in third-degree vertexes created by two hexagons (Figure 5).

There is a direct relationship between C_Y and C_{PA3} found by Dias[48−53] and presented in eq 7.

$$C_{Int} = C_Y + C_{PA3} \tag{7}$$

Pure cata-compounds (0% P_C), as a rule, present $C_Y = 0$ and $C_{PA3} = C_{Int}$, see eq 7. For pure peri-condensed and peri-condensed + cata-branches systems, the minimum value of C_Y is 2 and it increases by increments of 2 (Table 3). It is observed

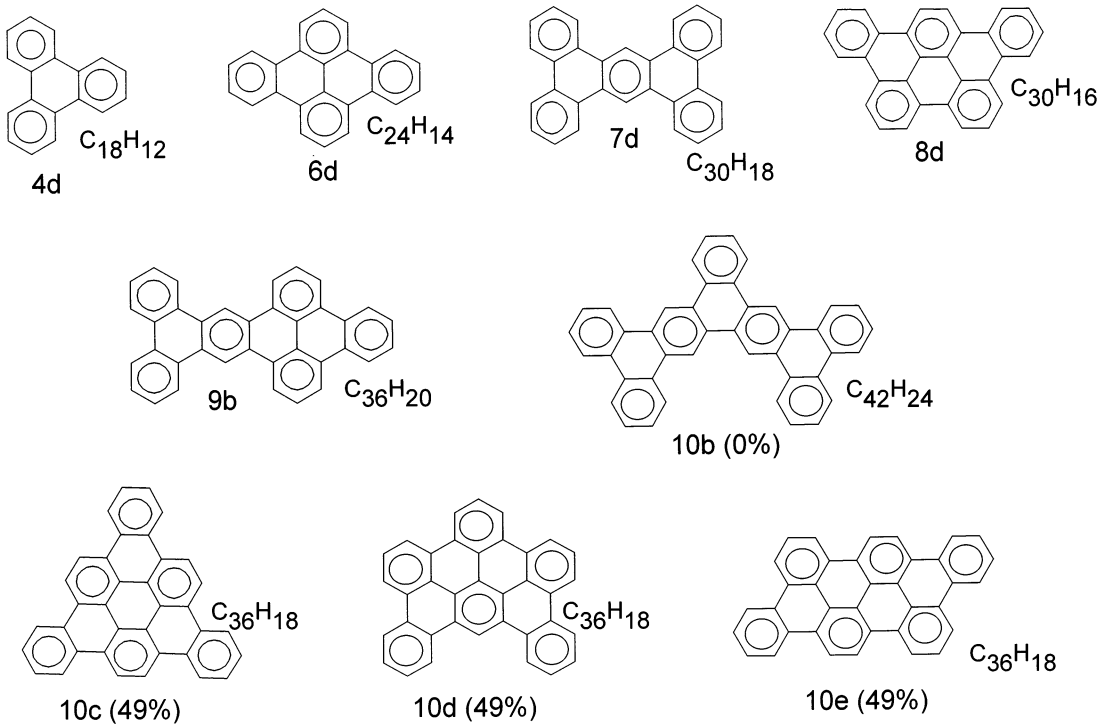

Figure 6. Compounds that present full resonant sextet structure and no localized double bonds. From 4FAR to 9FAR, there is only one isomer with full resonant structure. From 10FAR to 20FAR, there are more than one full resonant isomer for a given stoichiometry but those systems with P_C near to 70%−79% have only one full resonant structure. In this figure, only the full resonant sextet structures for 4FAR to 10FAR are drawn.

in Table 3 that as the degree of condensation increases also the value of C_Y increases while the value of C_{PA3} decreases and vice versa.

d_s, C_Y, C_{PA3}, and C_{Int} are structural elements that have fixed values within any given isomer set. These elements are related. With knowledge of the molecular formula of a PAH compound, it is possible to determine all of the structural information of the backbone, and the same applies for the fused rings regions in asphaltenes. With eq 2, C_{Int} can be calculated. The number of fused rings (nFAR) is calculated using eq 1, then C_Y is calculated with eq 8

$$C_Y = -2 + \text{nFAR} - d_s \tag{8}$$

d_s is a structural property that can also be deduced from Figure 1. All of the systems crossed by diagonal lines present the very same value of net number of disconnections among internal edges, d_s. It changes by one unit going from one row to another, see Figure 1. Finally from eq 7, C_{PA3} can be calculated. Also d_s can be calculated with eq 9. The relationships presented in eqs 8 and 9 were previously reported by Dias.[48−53]

$$d_s = C_{PA3} - \text{nFAR} \tag{9}$$

In Table 3 all the structural values for different stoichiometries for benzenoid PAHs are given. The d_s, C_Y, C_{PA3}, and C_{Int} values in Table 3 are the same for all of the isomers that belong to a same molecular formula and correspond to the structural features of the backbone only.

For a given stoichiometry in Table 3, there are many isomers that can be drawn. Dias[48−53] reported the number of isomers, and there is a recent supplement to Dias' work made by Cyvin and co-workers.[70] The number of PAH isomers increases rapidly with the increase of the number of fused rings, by many orders of magnitude (Table 3). The lower the percentage of compactness becomes, the higher the number of isomers is, and vice versa (Table 3). It would be impossible to study all of the isomers in many cases. But only some of the isomers are more stable and more likely to be good candidates for the fused ring region in asphaltenes. These are the strain-free benzenoid PAHs with a high number of resonant sextets.

By Clar's[29,30] sextet rule, a PAH compound containing a total resonant structure (TRS) or full resonant structure (FRS), that is, one that presents simultaneous sextets (three double bonds that in total involve six π-electrons and that are permutable within the same hexagonal ring), is the most stable (Figure 6). Each resonant sextet in a PAH structure adds roughly a stability of 36 kcal/mol (1.56 eV), as it is the case for benzene compared with cyclohexatriene, which has three localized double bonds.[71] Thus, of all of the isomers (Table 3), only some of them would be the most stable and possible structural candidates for the fused aromatic regions in asphaltenes. We will discuss which ones in the next sections.

The resonant sextets (N_R) or also called aromatic sextets are depicted by circle notation in all of our figures with chemical structures. The circle notation is used in its original formulation by Armit and Robison[40] rather than in its more common modern usage to depict delocalization. Any π electrons that do not participate in aromatic sextets are depicted as localized double bonds (Figures 2 and 3).

In Table 3 under the column of number of isomers, the number of full resonant structure isomers is given in parentheses, while in the N_R column, the total number of resonant rings or resonant sextets that can be reached in the full resonant structures is given under the label (full). The TRS has the characteristics that the simultaneous sextets occupy all of the carbons in the structure; therefore, there are no double bonds in any other region of the structure. Dias[72] has published a formula periodic table for total resonant sextet benzenoid hydrocarbons.

As we can see in Table 3, PAHs with both low and high P_C can have FRS isomers. In Figure 6, the structures of the FRS

for 4FAR to 10FAR are drawn. From 4FAR to 9FAR (Table 3), there is only one representative isomer having a full resonant structure within an isomer set. 5FAR has no full resonant structure isomer. The 5FAR structural series has two stoichiometries: $C_{20}H_{12}$ and $C_{22}H_{14}$ with 20 and 22 π-electrons, respectively. The π-electron content in each stoichiometry is not divisible by six. Dias[48,73a] has presented an aufbau process to obtain the more stable benzenoid isomers for PAH stoichiometries not having a π-electron content divisible by 6.

From 10FAR ahead, there are more than one full resonant isomer for a given stoichiometry. For example, for the structural series of 10FAR, $C_{36}H_{18}$ with 49% of compactness has 3 FRS isomers,[74] each one with six sextets ($N_R = 6$), which are presented in Figure 6. In contrast $C_{42}H_{24}$ (10FAR) with 0% of compactness has only one isomer with seven sextets, $N_R = 7$.

Coupling Clar's sextet rule with Fowler's leapfrog algorithm, Dias[73b] determined what type of nFAR would have a full resonant structure isomer(s). We found that for any FAR series those stoichiometries with $P_C \geq 80\%$ do not present full resonant structure(s) even if the counting of π-electrons is divisible by six. We were able to find easy equations (eqs 10 and 11) that allow us to calculate the minimum number of resonant sextets (N_R) for FRS in a FAR structural series. Equations 10 and 11 are used to determine for a FAR series which is the minimum resonant sextet number that will be presented in the smallest full resonant structure that might exist in that series. Then that minimum number of resonant sextets is associated with a stoichiometry by $N_R = C_A/6$.

$$N_R = 1 + \frac{\text{nFAR}}{2}$$

for even nFAR systems from 4FAR to 14FAR (10a)

$$N_R = \frac{\text{nFAR}}{2} \qquad \text{for even nFAR systems} \geq \text{16FAR} \quad (10b)$$

$$N_R = 1.5 + \frac{\text{nFAR}}{2}$$

for odd nFAR systems from 5FAR to 11FAR (11a)

$$N_R = 0.5 + \frac{\text{nFAR}}{2} \qquad \text{for odd nFAR systems} \geq \text{13FAR} \quad (11b)$$

The eqs 10 and 11 only provide the minimum value of N_R for the full resonant isomer(s) in a FAR structural series, which then is associated to the proper stoichiometry and from there the higher FRS with higher N_R can be associated with the corresponding stoichiometries, if applicable. In Figure 1, the subset of points corresponding to the stoichiometries with FRS are enclosed in a circle.

The FRS have an integer number of resonant sextets and no double bonds ($N_{DB} = 0$) in their structure, see Figure 6. However, all of the other PAH systems that are not FRS, linear, or zigzag (Figure 2) reach a maximum number of resonant sextets but present localized double bonds ($N_{DB} > 0$) in their structure. The highest number of resonant sextets (N_R) that these systems can present can be calculated with eq 12 and decreases by decrements of 1 until $N_R = 1$, which is the lowest value of resonant sextets in PAH systems that are not substituted.

$$N_R = \frac{(C_A - I_{even})}{6}, \quad I_{even} = 0, 2, 4, 6, \ldots \quad \text{until} \quad N_R = 1 \quad (12)$$

In eq 12, only N_R equal to an integer must be considered. From 7FAR, the N_R calculated with eq 12 cannot be reached if the structure has a $P_C \geq 79\%$; in this case only $N_R - 1$ can be reached. Thus, in the case of pure peri-systems, the highest number of resonant rings that can be present in the structure is related to the percentage of compactness or condensation.

Linear systems always present one sextet in the structure, and zigzag systems (Figure 2) present a number of resonant sextets given by eq 13.

$$N_R = 0.5 + \frac{\text{nFAR}}{2} \qquad \text{for odd nFAR} \quad (13a)$$

$$N_R = \frac{\text{nFAR}}{2} \qquad \text{for even nFAR} \quad (13b)$$

The total number of carbon atoms involved in resonant sextets will be denominated as C_{Ar}. The number of double bonds (N_{DB}) depending on the N_R in the structure can be calculated from eqs 14−16.

$$C_{Ar} = 6(N_R) \quad (14)$$

$$C_{DB} = C_A - C_{Ar} \quad (15)$$

$$N_{DB} = C_{DB}/2 \quad (16)$$

C_{DB} is the number of carbon atoms involved in localized double bonds. The number of resonant sextets and its corresponding number of double bonds for each stoichiometry from 2FAR to 10FAR are given in Table 3.

Table 3 summarizes the entire structural features for the backbone of the stoichiometries considered. Many relationship's can be derived from eqs 1−16, depending on the structural factors known of the PAH under study and therefore for the fused ring region in asphaltenes.

The C_{Int}, C_Y, C_{PA3}, and d_s structural factors calculated with eqs 2, 7, 8, and 9 only provide information about the structural features of the benzenoid PAH σ-backbones, that is, with no resonant sextets and no localized double bonds. When the resonant sextets and double bonds are incorporated into the structures, these values change, as we will discuss in detail in the following sections.

All of the structural features for free PAHs discussed in this section will be used in the discussion of the following sections.

5. HOMO−LUMO Gap in Free Polycyclic Aromatic Hydrocarbon Compounds

Mullins and co-workers[6,13,14] determined that the fluorescence emission spectra of asphaltenes represent the overlapping spectra of the many chromophores contained in the asphaltenes and that the spectral location of the fluorescence emission is related to the size of the chromophore. These researchers concluded that the bulk of asphaltene molecules possess one or two aromatic chromophores per molecule with 4−10 fused rings in each one. However, the distribution and structure of the fused rings in the chromophores in asphaltenes is largely unknown.

In this section, the theoretical HOMO−LUMO gap (the energetic gap between the highest occupied molecular orbital and the lowest unoccupied molecular orbital) for free PAHs is studied. The HOMO−LUMO gap and structural relationships of several PAHs are analyzed to draw conclusions about the distribution and structure of the fused rings in the aromatic cores of the chromophores in asphaltenes. All of the terms defined in

TABLE 4: Size, Molecular Weight, and HOMO−LUMO Energy Gap and Associated Wavelength for PAH Compounds with 4−14 Fused Aromatic Rings in Both Conformations, 0% of Compactness (linear and zigzag) and the Highest Pecentage of Compactness[a]

system	range of molecular size compact−linear (Å)[b]	formula (0% P_C)[c]	ΔE_{H-L} (eV) (0% P_C) zigzag molecule	ΔE_{H-L} (eV) (0% P_C) linear molecule	λ_{H-L} range (nm) (0% P_C) λ_{max} (nm) linear molecule	λ_{H-L} range (nm) (0% P_C) λ_{min} (nm) zigzag molecule	formula (highest P_C)	highest P_C, % (compd)	λ_{H-L} (nm) at highest P_C	ΔE_{H-L} (eV) at highest P_C
4FAR	9.24−11.94	$C_{18}H_{12}$	3.8632	2.8132	440.51	320.78	$C_{16}H_{10}$	100 (**4c**)	343.28	3.6100
			(3.4249[e])	(2.7276[e])	(454.33[e])	(361.83[e])			(335.41[f])	(3.6946[f])
			(3.4138[h])	(2.6089[d])	(475.00[d])	(363.00[h])			(333.50[g])	(3.7158[g])
									(375.76[e])	(3.2979[e])
									(374.00[h])	(3.3134[h])
									(373.00[i])	(3.3223[i])
									(365.00[j])	(3.3951[j])
5FAR	9.58−14.34	$C_{22}H_{14}$	3.6423	2.4028	515.75	340.23	$C_{20}H_{12}$	50 (**5c**)	439.55	2.8193
			(3.2871[h])	(2.3111[k])	(536.20[k])	(377.00[h])			(439.78[e])	(2.8178[e])
				(2.2834[l])	(542.70[l])				(440.00[h])	(2.8164[h])
				(2.1366[d])	(580.00[d])			(**5d**)	393.40	3.1500
									(405−410)[o,m,h]	(3.0598−3.0225)[o,m,h]
								(**5e**)	344.04	3.6020
									(377−382)[o,m]	(3.2871−3.2440)[o,m]
6FAR	9.57−16.67	$C_{26}H_{16}$	3.5661	2.2080	561.24	347.50	$C_{22}H_{12}$	82 (**6c**)	382.21	3.2423
									(399.81[e])	(3.0995[e])
									(405−410[i,m])	(3.0598−3.0225[i,m])
									(399.00[h])	(3.1058[h])
								(**6e**)	443.91	2.7916
									(434.57[e])	(2.8516[e])
									(436.47[p])	(2.8392[p])
									(431.00[i])	(2.8752[i])
									(432.00[h])	(2.8686[h])
7FAR	9.56−19.10	$C_{30}H_{18}$	3.5841	2.0849	594.39	345.76	$C_{24}H_{12}$	100 (**7c**)	422.34	2.9342
									(426.00[i])	(2.9090[i])
									(411.28[h])	(3.0131[h])
									(409.84[n])	(3.0237[n])
8FAR	11.43−21.63	$C_{34}H_{20}$	3.5281	1.8670	663.75	351.24	$C_{28}H_{14}$	75 (**8a**)	372.35	3.3281
									(430.00)[i]	(2.8819)[i]
								(**8c**)	402.71	3.0772
									(420.00)[i]	(2.9505)[i]
								(**8d**)	478.47	2.5899
								(**8e**)	617.14	2.0080
9FAR	11.42−24.07	$C_{38}H_{22}$	3.4454	1.7559	705.73	359.68	$C_{30}H_{14}$	89 (**9a**)	405.54	3.0557
								(**9c**)	508.57	2.4367
									(532.00[i])	(2.3294[i])
								(**9d**)	523.99	2.3650
10FAR	11.92−26.44	$C_{42}H_{24}$	3.4202	1.7152	722.48	362.33	$C_{32}H_{14}$	100 (**10a**)	438.79	2.8242
11FAR	13.70−28.85	$C_{46}H_{26}$	3.3754	1.6734	740.54	367.13	$C_{36}H_{16}$	83 (**11a**)	411.12	3.0143
12FAR	13.68−31.20	$C_{50}H_{28}$	3.3495	1.6422	754.62	369.97	$C_{38}H_{16}$	85 (**12a**)	414.99	2.9862
13FAR	13.68−33.54	$C_{54}H_{30}$	3.3487	1.6083	770.52	370.06	$C_{40}H_{16}$	99.8 (**13a**)	553.28	2.2410
14FAR	13.66−35.89	$C_{58}H_{32}$	3.3277	1.5728	787.90	372.40	$C_{42}H_{16}$	100 (**14a**)	496.54	2.4957

[a] All of the structures are optimized using the compass force field, and the transitions were calculated using ZINDO. Reported experimental results are in parentheses. [b] The size was measured considering the major longitude (longest dimension) in the molecule. [c] PAHs with linear and zigzag conformations have the same stoichiometry and 0% of compactness. [d] Reference 13. [e] Reference 61. [f] Reference 75. [g] Reference 76. [h] Reference 77. [i] Reference 54. [j] Reference 78. [k] Reference 79. [l] Reference 80. [m] Depending on the solvent. [n] Reference 81. [o] Reference 82. [p] Reference 108.

sections 4 and 4.1 (see above) will be used in this section. Refer to these sections when needed.

In a previous study,[58] to be published elsewhere, the validation of the method of calculation and of the calculated HOMO−LUMO gap (H−L gap) was carried out for 95 PAH compounds in which the calculated gap was compared with the reported experimental 0-0 fluorescence emission band. In this previous study, it was found that the structures optimized with the COMPASS force field yielded a result of the HOMO−LUMO gap that compares well with the experimental data. As the number of rings increases, there is a slight distortion from the planarity. From 9FAR on, this distortion is more significant, but in general, the structures are not concave. Semiempirical methods such as PM3 or AM1 produce a structure that is always planar despite the number of fused rings, and the calculated HOMO−LUMO gaps do not compare well with the experimental values.

In Table 4, the calculated HOMO−LUMO gap and associated wavelength for PAHs with 4−14 FARs are presented (for structures, see Figures 2, 3, 6, and 7) together with the available fluorescence emission experimental data. In this table, only the arrangements with a percentage of compactness of 0% (zigzag and linear), 100% (circular), and highest compactness for each FAR series are presented. As it can be observed in Table 4, there is an inverse relationship between ΔE and λ. The larger the ΔE value becomes, the lower the λ value is, and vice versa. There is, in general, a good agreement between theory and experiment with deviations of 33 nm (0.3149 eV) or less. The theoretical estimates are derived from a single "frozen" molecule in the gas phase at 0 K without corrections for thermal motions and solvent effects. The difference between the theoretical and experimental data could be due to the Stokes shift, which involves the reconfiguration of the solvent cage for the ground electronic state once the excited molecule of PAH

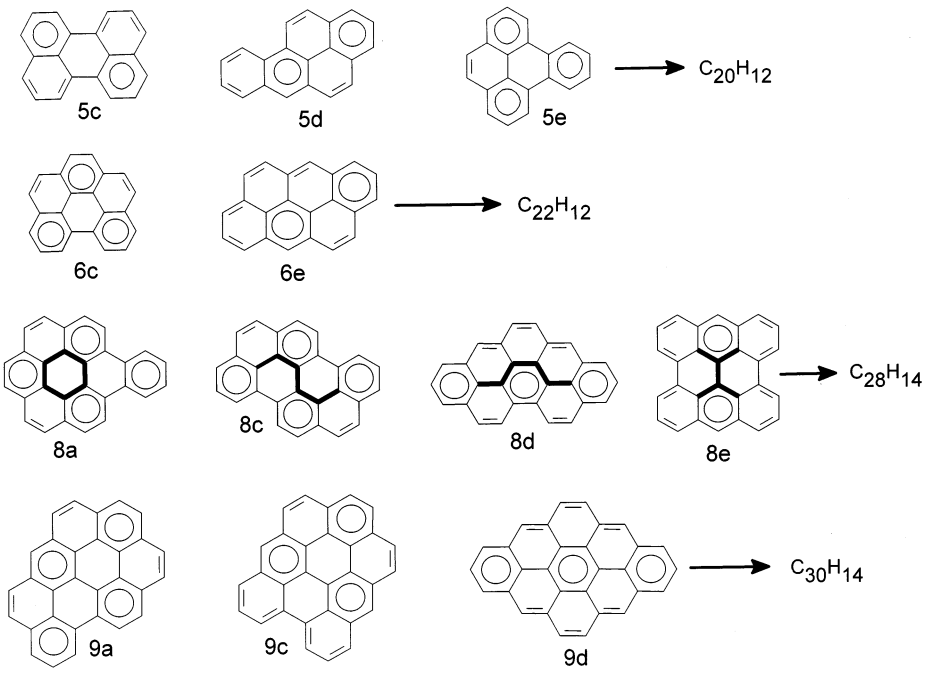

Figure 7. Structures of PAH compounds with highest percentage of compactness (P_C) from 5FAR to 9FAR.

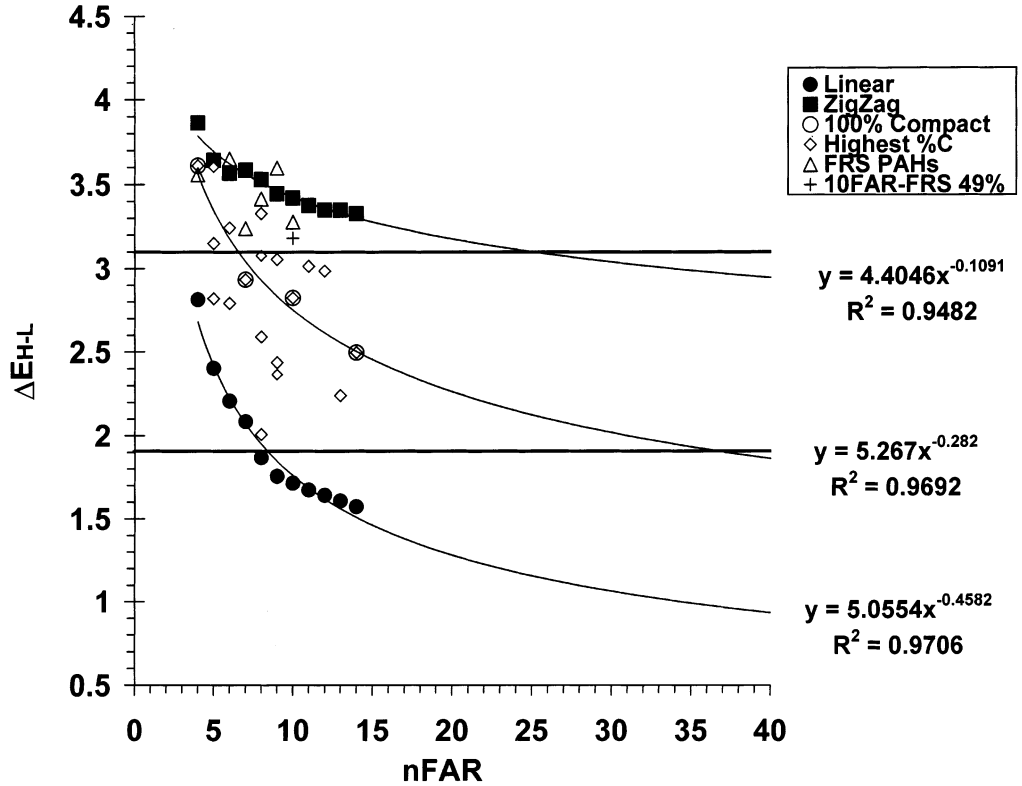

Figure 8. Diagram of ΔE_{H-L} versus the number of fused aromatic rings in benzenoid PAHs. All of the information presented in this diagram is in Table 4. The ΔE_{H-L} of linear, zigzag, circular ($P_C = 100\%$), and highest compactness structures is plotted. The two parallel thick lines delimit the experimental ΔE_{H-L} range observed for asphaltenes, which is reported to be 400−650 nm or 1.9065−3.0981 eV.[13] Fitting curves are shown. For any given nFAR, it is observed that the linear and zigzag structures present the lowest and highest ΔE_{H-L}, respectively. All of the other structures have ΔE_{H-L} that falls between these two limits.

undergoes photoemission.[62] In the case of 5FAR linear, the experimental results obtained by several groups vary up to 44 nm (0.1745 eV).

The agreement between theory and experiment is less satisfactory for **8a** (Figure 7, Table 4) with deviations up to 58 nm (0.4462 eV). The calculated gap of 3.3281 eV (Table 4) corresponds to a second singlet transition, which we identified in terms of the dominant singly excited configurations to correspond to the HOMO−LUMO transition ($C^2 = 0.71$). There is a first singly excited state at 424.28 nm (2.9208 eV), which corresponds to the dominant configurations (H − 1)−L ($C^2 = 0.45$) and H−(L + 1) ($C^2 = 0.48$). Thus, we consider that the experimental result of 430 nm (2.8819 eV) does not correspond to the so-assigned 0-0 fluorescence emission band.

All of the theoretical information given in Table 4 is presented in Figure 8 in a HOMO−LUMO gap (ΔE_{H-L}) vs number of

TABLE 5: HOMO−LUMO Energy Gap and Associated Wavelength for PAH Compounds with Full Resonant Structure (FRS) with Four Fused Aromatic Rings to Ten Fused Aromatic Rings[a]

system	formula	P_C (%)	structure	size (Å)	ΔE_{H-L} (eV)	λ_{H-L} (nm)	N_R	no of holes
4FAR	$C_{18}H_{12}$	0	**4d**	9.25	3.5574 (3.4963[b]) (3.5006[c])	348.35 (362.50[b]) (354.00[c])	1	3
6FAR	$C_{24}H_{14}$	33	**6d**	11.97	3.6504	339.48	2	4
7FAR	$C_{30}H_{18}$	0	**7d**	13.50	3.2384	382.66	5	2
8FAR	$C_{30}H_{16}$	45	**8d**	13.51	3.4146	362.92	3	5
9FAR	$C_{36}H_{20}$	16	**9b**	16.01	3.5970	344.52	6	3
10FAR	$C_{42}H_{24}$	0	**10b**	17.66	3.2773	378.12	3	7
10FAR	$C_{36}H_{18}$	49	**10e**	15.29	3.1813	389.53	4	6

[a] Experimental results are in parentheses. [b] Reference 61. [c] Reference 77.

fused rings (nFAR) diagram. It can be observed that the HOMO−LUMO gap increases going from the lowest P_C (linear, $P_C = 0$) to the highest P_C (most compact and circular structures), that is, from the highest stoichiometry to the lowest stoichiometry (Table 4 and Figure 8). However, the largest HOMO−LUMO gap corresponds to the stoichiometry with a zigzag structure that also has a 0% of compactness—highest stoichiometry and $C_Y = 0$. The lowest HOMO−LUMO gap corresponds to the completely linear structures. All of the other stoichiometries present a H−L gap that falls inside the linear−zigzag range. The H−L gap of the most compact structures (circular) falls inside the linear−zigzag range as well, Figure 8.

From 4FAR to 6FAR, there is an average change in the H−L gap between the zigzag and the linear structures of 1.4586 eV, while from 6FAR to 14FAR, there is an average change of 1.7420 eV (Table 4). The H−L gap of the full resonant structures (FRS) is comparable to the H−L gap of the zigzag structures, Figure 8. The H−L energy gap for the FRS is given in Table 5, and the structures are shown in Figure 6.

In Mullins' paper,[13] it is considered that by selection of excitation and emission wavelength, one can select a subset of chromophores. By comparing the experimental fluorescence emission of the 0-0 band of linear molecules from benzene to pentacene (5FAR), they concluded that short-wavelength excitation produces excitation of small chromophores (small number of fused rings) due to their large HOMO−LUMO gap. Correspondingly, long-wave excitation produces excitation of large chromophores (large number of fused rings) due to their short HOMO−LUMO gap. This statement has to be considered cautiously. Certainly, it is observed, and expected, that going from 4FAR to 14FAR there is a decrease in the HOMO−LUMO gap, or increase in λ, for any type of arrangement (zigzag, linear, circular, highest compactness) because we are moving toward a graphite type of structure (Table 4 and Figure 8). Highly aromatic graphite has a zero band gap.[84]

On the other hand, from Table 4 and Figure 8, it can be concluded that it is possible to have a small chromophore and a big chromophore—in terms of the number of fused rings—with a fluorescence emission in the same region. For example tetracene (**4b**), which is a linear (0% P_C) PAH with four fused aromatic rings, has a calculated H−L gap of 2.8132 eV (440.51 nm) and a calculated size (longest dimension) of 11.94 Å. Ovalene (**10a**), which is a circular (100% P_C) PAH with 10FAR, has a calculated H−L gap of 2.8242 eV (438.79 nm) and a size of 11.92 Å. Both PAHs present a fluorescence emission in the same region, and both have similar sizes.

Mullins and co-workers[13,14] concluded that there is a strong correlation between the size of the asphaltene chromophore, given by the emission wavelength, and the size of the molecule, given by the rotational correlation time.[13] In the case of our example, tetracene (**4b**) and ovalene (**10a**) have almost the same emission wavelength and also present the same sizes, in accordance with their conclusion. However, both compounds have very different number of fused rings, four in the case of tetracene (**4b**) and 10 in the case of ovalene (**10a**).

It could be argued that 10 fused rings and four fused rings are a small number of rings and because of that they fluoresce in the same range. However, there is a difference of six fused rings between tetracene (**4b**) and ovalene (**10a**). A 0-0 fluorescence emission band of 4.7[13] and 2.3 eV[79,80] is reported in the literature for benzene (one ring) and pentacence (five rings (**5b**)), respectively. There is a difference of 2.4 eV in the HOMO−LUMO gap and a difference of four rings between benzene and pentacene. Thus, the statement that short-wavelength excitation produces excitation of small chromophores and that, correspondingly, long-wave excitation produces excitation of large chromophores is only valid if by small or big chromophore reference to the size (longest dimension in Å) not to the number of fused rings is made.

As it can be seen in Table 4 and Figure 8, there is a change in the H−L gap given by the limiting structures linear and zigzag of 180 nm for 4FAR going from linear to zigzag and up to 400 nm for 14FAR. The extent of change in the H−L gap for the free PAHs presented in Table 4 encloses part of the range or the entire range, in some cases, of the fluorescence emission of asphaltenes, which is 400−650 nm or 1.9065−3.0981 eV.[13,14] The two horizontal bold lines in Figure 8 delimit the experimental fluorescence range of asphaltenes. It was not expected that for the same number of fused rings there could be a change in the HOMO−LUMO gap in average of 1.6 eV (290 nm) by changing the distribution of the fused rings in the space. The different distributions of the fused rings involve a change in the percentage of compactness (P_C, see section 4) and a change in the stoichiometry. However, for each stoichiometry, the percentage of compactness and the main structural features (d_s, C_Y, C_{PA3}, and C_{Int}, see section 4.1) are the same. Considering this last statement, it is not possible to explain why the zigzag structure (0% P_C and $C_Y = 0$) has the largest HOMO−LUMO gap and the linear structure has the shortest H−L gap (0% P_C and $C_Y = 0$) for a given FAR series. Both arrangements have exactly the same stoichiometry and the same structural characteristics in terms of d_s, C_Y, C_{PA3}, C_{Int}, and P_C, see section 4.1.

We consider that the change in the H−L gap for a same FAR series is more related to electronic features than to stoichiometrical characteristics, although all of them are interconnected. We refer to electronic features in terms of the number and location of resonant sextets in the PAH structures (N_R).

The consistent change in the HOMO−LUMO gap in each PAH series, which increases going from the linear arrangement to the most compact arrangement, is explained in terms of a consistent increase in the number of localized resonant sextets going from linear to circular. The zigzag structure should have among the highest number of resonant sextets and therefore the largest HOMO−LUMO gap and the highest kinetic stability (see Introduction). Thus, we consider that the zigzag PAHs, together with the full resonant PAHs, which have the largest HOMO−LUMO gap, present the highest number of resonant sextets in their structure, which makes them thermodynamically and kinetically more stable.

The density of the aromatic sextets (D_{as}) in a PAH structure, as Aihara[21] defines it, is given by eq 17.

$$D_{as} = \frac{C_{Ar}}{C_A} = \frac{6N_R}{C_A} \tag{17}$$

The D_{as} lies in the range of 0.0−1.0. The systems with a high number of resonant sextets in the structure have a D_{as} in the range of 0.75 to 1.00. The full resonant structures (FRS), which do not present localized double bonds in their structure, have a D_{as} value of 1.0. Only in the case of FRS, the circle notation to represent the aromatic sextets could be use to depict *delocalization* because all of the carbon atoms and all of the π density available are participating in the resonant sextets.

It can be observed from Figure 8 that the lowering in the H−L gap, when nFAR is increased, is more marked in the case of the linear arrangements than in the case of the zigzag arrangements. The linear structures have a D_{as} that approaches zero. This is because the linear systems only have one resonant sextet of which effect on the H−L gap is "diluted" as the total carbon content (C_A) is increased. Because of this, the H−L gap of the linear systems decreases faster than that one of the zigzag systems.

The PAH compounds with full resonant structure (FRS) (Figure 6 and section 4.1) present a H−L gap comparable in magnitude to the H−L gap of the zigzag structures. The FRS systems have the highest reachable number of resonant sextets in a FAR series. In Table 5, the H−L gaps for the FRS from 4FAR to 10FAR are given (Figure 6). The range of N_R goes from three (for 4FAR) to seven (for 10FAR, 49% P_C). All of the FRS present a H−L gap that is very similar. Their sizes are also similar, Table 5. All of the FRS are distorted from planarity because they present many bays (Figure 4, see section 4.1) that are near to each other causing the hydrogen atoms in the bays to be very closed. To find tendencies in the HOMO−LUMO gap, it is necessary to compare systems with a similar percentage of condensation.

The difference in the H−L gap between 4FAR (**4d**) and 10FAR (**10b**), both with 0% of compactness, is only 0.2801 eV, Table 5. A decrease in the H−L gap is expected going from 4FAR to 10FAR because we are moving toward a more graphite-like structure. However, it would be expected that the HOMO−LUMO gap of the 10FAR system would be smaller than it is only on the basis of the fact that the number of fused rings (hexagons or nFAR) is higher than that in 4FAR. But this is not the case because of the presence of seven resonant sextets ($N_R = 7$) in the 10FAR structure, compared with three resonant sextets ($N_R = 3$) in 4FAR, which provides a higher kinetic stability that opens the H−L gap. This supports again the fact that it is incorrect to consider that big chromophores (in terms of number of FAR) have small H−L gaps and that small chromophores have large H−L gaps. However, the effect of the seven resonant sextets in the 10FAR structure was not enough to produce a gap bigger than that of the 4FAR gap. There are other structural factors besides the number of fused aromatic rings and number of sextets that must be considered and that together counteract part of the effect on the H−L gap by the presence of the seven resonant sextets. One of these factors might be the presence of three "holes" or "empty rings" in the 10FAR structure, **10b**, compared to one "hole" in the 4FAR structure, **4d**. To quantify the effect on the HOMO−LUMO gap of the empty rings, a theoretical systematic study would have to be carried out.

Although we could consider that there is a delocalization of π density in the entire full resonant structures, it is only possible to reach the highest number of resonant rings if they are localized in specific hexagons in the structure. However, despite this localization of resonant rings in the FRS, all of the π electrons and all of the carbon atoms are involved in resonant sextets. It is possible to talk about "holes" or "empty rings", if the resonant sextets are localized.

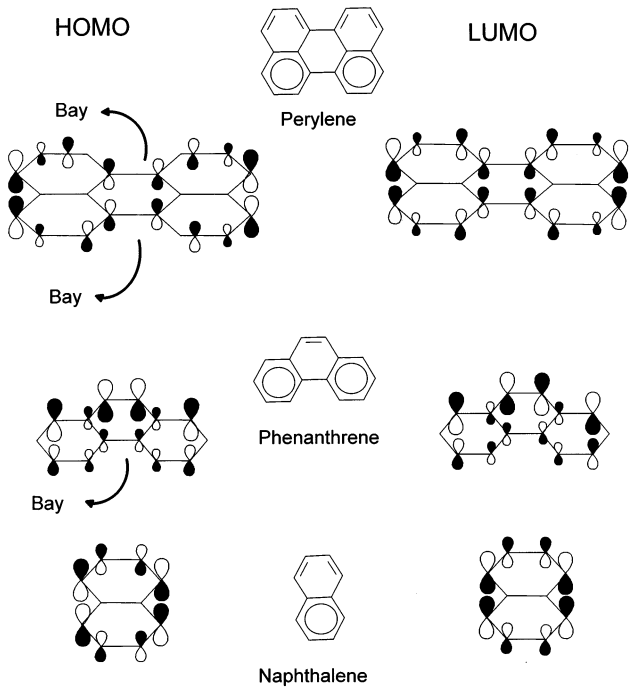

Figure 9. Schematic representation of the HOMO and LUMO molecular orbitals of perylene, phenanthrene, and naphthalene.

To understand the effect of the presence of holes in the PAH structures, we could look at the case of perylene, **5c**. Perylene, **5c**, has one hole in the structure (Figure 9). This hole is located in the central hexagon, which comprises two bay regions. The HOMO and LUMO of perylene are quite different from those of phenanthrene (Figure 9), especially in their bay regions.[85] Phenenathrene has one bay and no hole in the structure.

The HOMO of perylene, Figure 9, has been described as the out-of-phase combination of the HOMO of naphthalene and the LUMO of perylene as the in-phase combination of the LUMO of naphthalene (Figure 9).[85] In this way in the LUMO of perylene, there is a bonding contribution in the hexagon that involves the hole while in the HOMO there is an antibonding interaction. Thus, the HOMO and the LUMO are destabilized and stabilized, respectively, with respect to naphthalene.

The stabilization or destabilization of the frontier orbitals, as we can see, depends on several factors, which are the number of fused rings, the number of resonant sextets present in the structure, the number of holes present in the structure, and the PAH edge structure (this last factor will be discussed in section 6). All of these factors are interconnected, and to understand the effect of all their possible combinations on the HOMO−LUMO gap in PAH is not an easy task.

Now comparing the HOMO−LUMO gap of the FRS, Table 5, with a similar compactness but greater than zero, we observed that the full resonant structure with 10FAR and 49% of compactness, **10e**, presents the smallest H−L gap and 6FAR (**6d**, $P_C = 33\%$) has the largest H−L gap. 10FAR has six resonant sextets and four "holes", while 6FAR has four resonant sextets and two "holes", Figure 6. There is a difference of 0.4691 eV in the H−L gap between these two systems. 10FAR has a H−L gap of 3.1813, and 6FAR has a H−L gap of 3.6504 (Table

5). On the other hand, 8FAR (**8d**, $P_C = 45\%$) has a H−L gap that is between these two values, 3.4146. 8FAR has five localized resonant rings and three "holes".

On the basis of the fact that the presence of resonant sextets confers stability to the structure and opens up the HOMO−LUMO gap, we would expect that the HOMO−LUMO gap of 10FAR with six resonant sextets would be larger than the HOMO−LUMO gap of 6FAR, which has four resonant sextets. However, this is not the case. We attribute that the higher number of holes and fused rings in 10FAR diminishes the stabilizing effect of the six resonant sextets.

The FRS systems have the highest reachable number of resonant sextets in their structure compared with other PAH and always present holes, which is not necessary the case with other PAH. It seems to be a correlation between the number of fused aromatic rings, the number of resonant rings, the number of holes, and the H−L gap. On one hand, the presence of resonant sextets opens the H−L gap up, but on the other hand, the presence of holes seems to close the H−L gap. The effect on the H−L gap of the presence of a high number of holes is strong, and it is more accentuated in the case of FRS.

In Tables 4 and 5, the calculated size (longest dimension) of the studied systems is also presented under the column of molecular size. In this column, the size of the compact (peri) and linear structures (cata) for the given FAR are provided. The peri and cata compounds for a given FAR have different stoichiometries and represent the limiting sizes. All of the other possible stoichiometries and structures have sizes that fall within these two limits. The size of the optimized structures was measured considering the major longitude in the optimized molecule. Using asphaltene rotational correlation times, Mullins and co-workers[13] reported an experimental size of the whole asphaltenes to be 10−20 Å with molecular weights in the range of 500−1000 g/mol. Scanning tunneling microscopy (STM),[20] which is sensitive only to the size of the aromatic fused region in asphaltenes, quoted a mean value of the aromatic ring region of asphaltenes to be 10 Å in diameter, which is roughly 40% of the whole size of an asphaltene molecule.

The range in size for 10 fused rings from a compact circular arrangement to a linear one spans from 11.92 to 26.44 Å (Table 4). The sizes of all of the other systems with different percentages of condensation fall between these two limits.

The size of 10 fused rings in the most compact arrangement (ovalene, **10a**) is calculated to be 11.92 Å. The size of 11 fused rings in the most compact arrangement (**11a**) is calculated to be 13.70 Å, Table 4. Thus, only on the basis of size criteria, we conclude that asphaltenes have 4−10 fused rings in their fused ring region. However, the arrangement of 10FAR would have to be highly compact (with high percentage of compactness) to be near the experimental asphaltene size. Beyond 10FAR, the calculated size is bigger than the observed experimental size.[13]

If an asphaltene molecule contains a single four fused ring region (4FAR) with 40% of the carbon being part of its ring region (STM results[20]), then the molecular weight of the whole asphaltene would be around 505 to 570 g/mol for circular and linear arrangements, respectively. On the other hand, if an asphaltene molecule contains a single 10 fused ring region (10FAR) with 40% of the carbon being part of its ring region, then the molecular weight of the whole asphaltene would be around 995 to 1125 g/mol for circular and linear arrangements, respectively. Beyond 10 fused ring regions, the molecular weight would be bigger than the experimental molecular weight of 500−1000 g/mol.[13]

By size and weight considerations (Table 4) and taking into account the experimental results,[13,20] we conclude that the fused region(s) in asphaltenes present four to nine maybe 10 fused rings in each individual aromatic system. By size, we conclude that the linear structures are not possible candidates for the fused ring region in asphaltenes (Table 4) and the circular structures are possible. By weight considerations from 4FAR to 10FAR, linear or compact structures are possible. The conclusion reached about the number of fused rings in the fused ring region in asphaltenes using the calculated sizes agrees with the experimental results found by Mullins and co-workers.[13]

The most important consideration to finally conclude about the exact distribution of ring sizes in each chromophore or at least to reduce the range of possibilities is given by the fluorescence emission of asphaltenes. The two horizontal bold lines in Figure 8 delimit the experimental fluorescence range of asphaltenes. We conclude that the zigzag structure is not possible for the fused ring region(s) in asphaltenes because from 4FAR to 10FAR the HOMO−LUMO gap does not fall into the asphaltene experimental range. We performed a curve fit, which is presented in Figure 8. The best curve that we could fit is a potential equation with $R^2 = 0.9482$, which is reasonable. With this curve, we predict that the zigzag structures will fall into the asphaltene experimental range from 25FAR ahead. However, 25 fused aromatic rings in zigzag distribution would have a size and a weight that is out of the experimental results for asphaltenes.

In the case of linear structures only from 4FAR to 7FAR, the H−L gap falls into the experimental range of asphaltenes, Figure 8. We found the best curve that predicts the H−L gap of linear systems in terms of the number of fused rings (nFAR). The equation is given in Figure 8. It is reported in the literature[86] that petroleum asphaltenes are peri-type. This characteristic does not correspond with a linear structure. Thus, we conclude that the fused ring region in asphaltenes cannot have linear structure.

Only the HOMO−LUMO gap of the linear arrangement of the 4FAR series falls into the experimental range of asphaltenes. None of the other 4FAR arrangements fall into the experimental range of asphaltenes. Thus, four fused aromatic rings in any arrangement are not good structural candidates for the fused aromatic ring region in asphaltenes.

The full resonant sextet structures have a HOMO−LUMO gap that is comparable with the one of the zigzag structures (Figure 8) and do not fall into the experimental range of asphaltenes. As discussed before, these structures have the highest number of resonant sextets in their structure and they are the most stable. This stability is reflected in a large HOMO−LUMO gap. We conclude that the structure of the fused ring region in asphaltenes cannot be of the full resonant structure type despite the percentage of condensation (Table 5, Figure 6).

As it can be seen in Figure 8, the HOMO−LUMO gap of the full resonant structures does not decrease gradually going from 4FAR to higher number of fused aromatic ring systems. There is an oscillation of the H−L gap as the number of fused aromatic ring increases. The H−L gap goes up, reaches a maximum value, and then goes down until a minimum value, and it goes up again, as the number of nFAR is gradually incremented.

For the case of circular systems with percentage of condensation of 100%, we conclude that the circular structure of 7FAR (coronene, **7c**) and 10FAR (ovalene, **10a**) are possible structural candidates for the fused ring region(s) in asphaltenes, for the reason that their HOMO−LUMO gap falls into the asphaltene

experimental range but any other circular structure is not possible (Figure 8). The size (longest dimension) and weight of pure peri-condensed PAH ($P_C = 100\%$) beyond 10FAR do not fall into the experimental range reported for asphaltenes.

6. The Oscillation of the HOMO−LUMO Gap in PAHs

The oscillation of the H−L gap is observed for all of the systems that are not linear (0% P_C), zigzag (0% P_C), or circular (100% of compactness), that is, for FRS and peri-systems, as the number of fused aromatic rings is increased. However, the oscillation of the HOMO−LUMO gap always falls into the zigzag−linear limiting region, Figure 8.

The oscillation of the HOMO−LUMO gap has been previously observed.[85,87] It has been reported that the electronic properties of highly condensed polynuclear aromatic PAHs depend on their molecular sizes and edge structures.[65−69] Two main edge structures have been identified: the phenanthrene-edge-type and the acene-edge-type, Figure 4. It has been concluded that the characteristics of the frontier orbitals significantly depend on the edge structures of highly condensed polynuclear aromatic PAHs.[67,69] Also the Dewar's resonance energy[88] has been correlated with the edge structure of PAHs.[65]

The topological factors governing the HOMO−LUMO gap of ladder polymers were analyzed by Hosoya and co-workers.[89] These authors discussed that polyacene and polyphenanthrene can be viewed as interacting *trans*-polyene chains and *cis*-polyene chains, respectively. When the chain width is increased by increasing the number of polyene chains (n), it is observed that H−L gap of the acene-edge series decreases very rapidly, while the H−L gap of the phenanthrene-edge series approaches zero very slowly with n in an oscillating manner with a behavior that has a periodicity of 3 in n.[90]

Yoshizawa and co-workers[85] classified the phenanthrene-edge polymers, PPh(n), in three main groups—the small-gap (metallic) group, PPh($3m + 1$), large-gap group, PPh($3m + 2$), and medium-gap group, PPh($3m$), in which $m = 0, 1, 2, 3, ...$—and explained the oscillating behavior in the H−L gap of the three groups from the viewpoint of interchain interactions in the frontier crystal orbitals. In our study, we observe an oscillation of the H−L gap in terms of the number of fused aromatic rings (nFAR) and in some cases in terms of the percentage of compactness (P_C). We found that the oscillation of the H−L gap has a periodicity of 2 in full resonant structures, FRS. On the other hand, in structures with the highest compactness P_C, different to 100%, the periodicity is 3.

In Figure 6, the full resonant structures (FRS) from 4FAR to 10FAR are depicted. All of these systems possess a single resonance structure, which involves the largest possible number of aromatic sextets. Structures **4d**, **6d**, **8d**, and **10e** (Figure 6) have the same topological characteristics in terms of edge structure and belong to the same group. It can be observed in Figure 8 how the H−L gap of this group is decreasing as the number of nFAR is increased. Thus the periodicity in the decreasing of the H−L gap for this group is 2. In this group, the number of localized resonant sextets, number of empty rings or holes, and the number of bays increase as nFAR increases. The decrease in the H−L gap is smooth, Figure 8. All of these structures have a cis edge, (Figure 4).

It is possible to divide the structures with highest percentage of compactness, P_C, and the pure peri-condensed circular structures ($P_C = 100\%$) enclosed in the zigzag−linear region (Figure 8) by groups, PAH(nFAR). The values of the HOMO−LUMO gap decreases monotonically for each group. We found that some PAH molecules belong to more than one group. The systems with percentage of compactness equal to 100% belong to the same group. We could say that there is no periodicity in the reduction of the HOMO−LUMO gap for these systems because the HOMO−LUMO gap decreases as the number of fused aromatic rings increases. The 100% P_C circular systems, PAH(nFAR = 4, 7, 10, 14, 19, 24, ...) are those that fall on the upper limit curve in Figure 1. These have the characteristic that their edge is of the type trans edge, Figure 4.

A closer look at the highest P_C systems including also $P_C = 100\%$ systems allows us to divide them into groups. Some of the possible groups have only cis edges or trans edges (Figure 4), but there are systems with combinations of both types of edges in which bays are presented in different numbers. The values of the HOMO−LUMO gap decrease monotonically for each group. We will focus on the systems in which H−L gap falls in the zigzag−linear region and that have highest P_C or 100%, Figure 8.

The PAH($3m + 1$), $m = 1, 2, 3, ...$, group encloses PAH(4) (**4c**), PAH(7) (**7c**), PAH(10) (**10a**), PAH(13) (**13a**), PAH(16), ..., Figure 3, Figure 8, and Table 4. All of these systems have in common that their edge is of trans-edge-type or acene-edge-type (Figure 4) and they do not present bays in their structure. The oscillation of the HOMO−LUMO gap has a periodicity of 3. In Figure 8, it can be seen that the HOMO−LUMO gap for this group decreases rapidly. Pyrene (4FAR, **4c**) has two localized resonant rings (N_R) and no holes in its structure, coronene (7FAR, **7c**) has $N_R = 3$ and one hole, ovalene (10FAR, **10a**) has $N_R = 4$ and three holes, and 13FAR, **13a**, has also $N_R = 4$ and four holes. As it can be in Figure 8, the decrease in the H−L gap from 7FAR to 10FAR is smooth but there is a jump from 10FAR to 13FAR. This is because 13FAR has four resonant rings, as does 10FAR, and in the case of 13FAR the stability that the resonant rings can confer to the structure is diluted provoking a sharp decrease in the HOMO−LUMO gap. What all of these structures have in common is that they have a trans edge structure and they are constructed by adding phenanthrene fragments to the pyrene core. Also, the number of empty rings or holes increases as nFAR is increased.

The other two groups that can be identified are the PAH-(nFAR = 5, 8, ...) (**5e**, **8a**) with a periodicity of three in the decrease of the HOMO−LUMO gap, and the group PAH(nFAR = 6, 9, ...) (**6c**, **9c**) with also a periodicity of 3, see Figure 7 and Figure 8. The structures in these groups have similar edges and building blocks.

By dividing the PAH compounds into different groups with similar characteristics in terms of edge structure, it is possible to identify the decreasing behavior of the HOMO−LUMO gap in each group. It is true that for each different group the larger systems will have a lower H−L gap (associated with a higher wavelength) and the small systems will have a larger H−L gap (associated with a smaller wavelength). However, in the case of the fluorescence spectrum of asphaltenes, which involves the overlapping spectra of the many chromophores contained within the asphaltenes,[13] members of different groups might be excited and they can vary in sizes and number of resonant sextets in their structures. Thus, chromophores observed at short or long wavelengths not necessarily are small or big in size.

In each group, the HOMO−LUMO gap decreases slowly or quickly depending on the number of localized resonant sextets and the number of holes in the structures. A more detailed study of the different groups involved in the oscillation of the HOMO−LUMO gap would require a more complete theoretical study in which more isomers and more nFAR are included. Aihara[21] pointed out before that many different homologous

series are conceivable for PAH molecules, which are substructures of benzenoid polymers, and that their HOMO−LUMO gap is closely related to their aromaticity, which is related to the density of aromatic sextets in the structures.

7. The Aromatic Fused Region in Asphaltenes

In section 5, it was concluded that asphaltenes have five to nine, maybe 10, fused rings in their fused ring core. It was concluded that the arrangements of the fused ring region cannot be linear or zigzag or have a full resonant structure. In the case of circular arrangements, asphaltenes might have a coronene (7FAR, $P_C = 100\%$, **7c**) and ovalene (10FAR, $P_C = 100\%$, **10a**) type of structure only. Petroleum asphaltenes are reported to be of the peri-type with cata-branches. Thus, the circular structures might not be after all possible.

In this section, we will discuss all of the other possible arrangements of the fused ring region in petroleum asphaltenes, that is, the arrangements with a percentage of compactness different from 0% and 100% and that are not of the full resonant type despite the percentage of compactness.

Some of the peri-systems with the highest percentage of compactness different from 100% (Figures 3 and 7), points marked with diamond symbol in Figure 8, have a HOMO−LUMO gap that falls into the experimental range of asphaltenes. Each nFAR has a number of isomers for the highest percentage of compactness. The number of isomers is reported in Table 3.

In Table 3, it can be seen that 5FAR has three isomers ($P_C = 50\%$), 6FAR has two isomers ($P_C = 82\%$), 8FAR has eight isomers ($P_C = 75\%$), and 9FAR has three isomers ($P_C = 89\%$). We did not calculate all of the possible isomers from 10FAR ahead. In Figure 7, the structures for the isomers studied herein are presented. For 8FAR ($C_{28}H_{14}$), we only calculated four isomers instead of the eight that exist; however, these four isomers are representative of the rest. These 8FAR compounds with 89% of compactness can have four, three, and two resonant rings in their structure, Table 3. We have calculated one isomer for each case, Figure 7.

The isomers with the highest number of resonant rings do not fall into the experimental fluorescence emission range of asphaltenes (Table 4 and Figure 8). These isomers are **5e**, **6c**, and **8a** (Table 4, Figures 7 and 8). The isomer **9a**, which exhibits the highest number of resonant sextets, is very near the upper experimental limit, yet it falls into the experimental range. The same is observed for **8c**.

On the other hand, **8e** is very near to the lower limit of the asphaltenes experimental fluorescence emission and near to the linear curve, Table 4 and Figure 8. Isomer **8e** has the lowest number of resonant rings therefore lower stability, which is reflected in a lower HOMO−LUMO gap. Isomer **8e** could be described as two linear anthracene molecules interacting, and it might be that because of this the HOMO−LUMO gap of this system is near to the linear curve, Table 4 and Figure 8. The HOMO of perylene (**5c**) has been viewed as the out-of-phase combination of the HOMO of naphthalene and the LUMO of perylene as the in-phase combination of the LUMO of naphthalene.[85] We note that the HOMO−LUMO gap of **5c** is also near to the linear curve, Table 4 and Figure 8.

We can say that **8a** and **8c** are structurally very similar. These compounds have four localized resonant sextets, two bay regions, two empty hexagons or holes, and two localized double bonds, Figure 7. However, there is a difference in the HOMO−LUMO gap of 0.2509 eV (30 nm) between them. We consider that this is not a big difference and it could be attributable to the ratio between the number of duo groups (η_2) and the number of solo (η_1) groups in each compound (Figure 4 and section 4.1). Isomer **8a** has an η_1 to η_2 ratio of 0:5, while **8c** has a 0:4 ratio. It seems that there is an extra stability in the HOMO−LUMO gap when the values of η_1 and η_2 are closer. Also the stability of a PAH structure is decreased when in the structure there are present bays or coves or fjords, by the order bay < cove < fjord, because of steric hindrance between hydrogen atoms in these regions (Figure 4).

Peri-compounds with a difference between η_1 and η_2 equal to 4 from 5FAR to 8FAR seem to have a HOMO−LUMO gap that falls into the experimental fluorescence emission range of asphaltenes. On the other hand, for 9FAR systems, it seems that PAH compounds with a difference of 5 between η_1 and η_2 have a HOMO−LUMO gap that falls into the experimental fluorescence emission range of asphaltenes.

The HOMO−LUMO gap of **8a** is out of the experimental fluorescence emission range of asphaltenes because the difference between η_1 and η_2 is equal to 5, while **8c** has a difference of 4, and its H−L gap falls into the experimental range. The difference in the HOMO−LUMO gap between **8c** and **8d** is 0.4800 eV and 0.5819 eV between **8d** and **8e**. All of these systems have the formula $C_{28}H_{14}$ and a percentage of compactness of 75%, and the number of resonant rings for this stoichiometry is four, three, and two (Table 3). Thus, **8a** and **8c** must have four resonant sextets, **8d** three, and **8e** two. The H−L gap range of these 8FAR systems span a range of 1.32 eV (244.79 nm), from two resonant rings (**8e**) to four resonant rings (**8a**), which can be considered as a large range. The HOMO−LUMO gap is seen to decrease as the number of resonant rings decreases.

By comparison of the HOMO−LUMO gap between **8c**, **8d**, and **8e**, all falling into the experimental fluorescence emission range of asphaltenes, it is observed that in general the increase of the number of resonant sextets by one in structural isomers opens up the HOMO−LUMO gap by approximately 0.4−0.5 eV.

It is interesting to notice that the positions of the resonant rings, which we draw as a natural choice to fulfill the valency, are in the hexagons that have the carbons with a connectivity of three, that is, the Y-carbons (C_Y) (Figure 5). The 8FAR systems **8a** and **8c**−**8e** have $C_Y = 6$, and the location of the resonant rings in each isomer fulfills this property. It seems that C_Y provides information about the location of the resonant sextets in the peri-section in PAHs. C_Y is also related to the possible number of resonant rings that can be drawn in a particular structure, and it can give an idea of the magnitude of the expected H−L gap, if information on any other isomer is known. For example, in **8e**, the six internal Y-carbons that define C_Y are located in the central hexagons of each anthracene fragment, Figure 7. The maximum number of resonant rings that can be drawn for this structure is two to fulfill the valencies. The resonant sextets can be placed in the external hexagons of each anthracene fragment (which will involve $C_Y = 2$) or one sextet in an external hexagon of one of the anthracene fragments and the other in the central hexagon of the other anthracene fragment (which will involve $C_Y = 4$). Or the last possibility is to locate the two resonant rings at the central hexagon of each anthracene fragment (which will involve $C_Y = 6$). Isomer **8e** and perylene (**5c**) can be considered to be members of a group. Isomer **8e** has two anthracene fragments, and **5e** has two naphthalene fragments. It is reported in the literature that in perylene (**5c**) the π-density is located in naphthalene fragments and distributed in the same way as in naphthalene.[91] Thus, we consider that in the case of **8e** the two resonant rings will also

be located in the polyacene fragments and in the same way as in anthracene. It is reported that anthracene has only one resonant sextet located in the central hexagon.[47,92] Thus, the location of the two resonant sextets in **8e** involves the carbons that define $C_Y = 6$.

5FAR has three isomers (Figure 7). The HOMO−LUMO gap of **5e** does not fall into the experimental range for asphaltenes, the H−L gap of **5d** is near the upper experimental line, and the H−L gap of **5c** falls into the experimental range. The three compounds have the same stoichiometry and the same percentage of compactness; however, the difference in the HOMO−LUMO gap is 0.7827 eV (95.51 nm) between **5c** and **5e** (Table 4).

The differences between these three isomers are the structural characteristics. These three isomers have the formula $C_{20}H_{12}$ and 50% of compactness. The maximum number of resonant sextets for this stoichiometry is three, and the minimum is two (Table 3). Thus, **5e** must have the highest number of resonant rings, that is, three, while **5c** must have the lowest number of resonant rings, that is, two. The difference in the HOMO−LUMO gap is 0.3307 eV between **5c** and **5d** and 0.4520 (eV) between **5d** and **5e**, Table 4. Again it seems that the increment of one resonant ring has the effect of opening up the HOMO−LUMO gap by around 0.4 eV.

The H−L gap of **5d** is higher than the one of **5c** by 0.3307 eV. This is not a value that could be related to the effect of one more resonant ring. But it could be due to the fact that in **5d** the two hexagons containing the resonant rings are bonded together while in **5c** they are apart and there is an empty hexagon or hole between them and because of this the stability is lowered in **5c**. Using molecular electrostatic potential topography calculations,[93] Suresh and Gadre found that in benzanthracene the resonant rings prefer to be located in hexagons that are bonded as in polyphenyls. Infinitely large polyphenyl compounds have a large HOMO−LUMO gap.[21]

If it were true that the increment of one resonant ring between isomers opens up the HOMO−LUMO gap by approximately 0.4 eV, then we would expect a difference of 0.4 eV between the H−L gap of **5c** and **5e**. Instead, the difference is almost the double, 0.7827. We believe that the arrangement of the resonant rings has an effect of increasing or decreasing the stability in the isomers. It seems that the arrangement of the hexagons that contain the three resonant rings in a "triphenylenic unit", as in **5e**, confers an extra stability of approximately 0.4 eV more. It has been reported in the literature that the resonant rings in triphenylene (**4d**) are localized and they are in the external hexagons.[92,94] The resonant rings in the three isomers (Figure 7) are located in hexagons that involve the internal Y-carbons. For these three isomers, $C_Y = 2$. Again the Y-carbons provide information about the location of the resonant sextets in the peri-section in PAHs.

Isomer **5e** is an example of a peri + cata-branch compound. The peri region has two resonant rings in the hexagons with the Y-carbons. After placing these two rings, there is only one possibility of drawing the third resonant ring keeping the valence of carbon and it is in the external hexagonal that shapes the cata-branch.

The same type of analysis could be done for the 6FAR isomers and 9FAR isomers presented in Figure 7. In general, the structural isomers with more resonant sextets will have a higher HOMO−LUMO gap than the isomers with less resonant sextets in the structure.

As we discussed in the Introduction, the fused ring region(s) in asphaltenes contain heteroatoms (N, O, S). Our study of PAHs does not include heteroatoms. It is known experimentally that the replacement of carbon in PAH compounds with heteroatoms typically results in red shift (higher wavelength) of the fluorescence maximum, if there is any spectral effect.[61,62] Thus, those systems with a HOMO−LUMO gap slightly above the upper border line of the experimental range of asphaltenes, as it is the case of **5d**, might fall into the experimental range when a heteroatom is added to the structure. However, the HOMO−LUMO gap of **8e** might go out of the experimental range of asphaltenes when a heteroatom is added to the structure. We are extending our study to the effect of heteroatoms (S, N, O) on the HOMO−LUMO gap of the PAH systems already studied.

After all of the exposed facts, we could say that there is an over use or abuse in the drawing of the resonant sextets in PAH compounds and in the fused ring region(s) in asphaltenes. It is a common use to draw resonant rings all over the place in the PAH structures, which in the case of asphaltenes can lead to erroneous conclusions. It is believed that asphaltenes might interact among them by $\pi-\pi$ interactions forming stacks because it is argued that there is a uniform π cloud, as in benzene, above and below the carbon sheet. This would be completely true for the case of FRS PAHs but not for the other PAHs in which the resonant sextets and the double bonds are localized in certain regions modifying in this way the kinetic stability and reactivity, including aggregation, of these PAHs. As exposed in section 5, FRS is not possible for asphaltenes.

^{13}C and ^{1}H NMR studies of asphaltenes provide good information about the number of aromatic carbons and hydrogen atoms bonded to them. However, NMR experimental studies cannot provide information about which carbon atoms are part of localized resonant sextets. In a very complete review made by Lazzeretti[95] about the ring currents, he concludes that proton chemical shift does not seem to provide the best proof of the existence of ring currents. On the other hand, the experimental determination and analysis of the components of the ^{1}H and ^{13}C NMR tensors is complicated in some cases, and at the present time, it is not possible for asphaltenes. The analysis of the NMR tensor components has provided information about the localization of the π-electrons in PAHs.[91,94] However, the analysis has been complicated.

The only molecule for which the unique proton shielding indicates the existence of ring current, as the current generated by the existence of a resonant sextet involving six π-electrons in movement, is benzene. The experimental ^{1}H NMR for benzene is 7.42 ppm.[96−98] The H atoms of benzene are bonded to aromatic carbons (H_{Ar}) in the sense that they are bonded to carbon atoms that form part of a resonant sextet. The reported experimental ^{13}C NMR for benzene is 128.2 ppm.[99] All of the C atoms are aromatic (C_{Ar}). For the fused ring region in asphaltenes is reported that H appears in the range of 6.5−9.0 ppm and C appears at 100−170 ppm.[63] The experimental range reported for asphaltenes is too wide to conclude that the C and H atoms in the fused ring region are all aromatic, that is, ones that form part of resonant sextets. In some cases, it is known that the displacement of NMR signals could be due to a paramagnetic current localized in adjacent fragments.[100] Thus, the observed signals could arise from the overlapping of paramagnetic currents coming from near-resonant sextets.

As it was previously concluded by Suresh[93] and co-workers, only benzene has a perfect six π-delocalization, which is intimately connected with its high symmetry, whereas the hexagonal rings of all of the annelated systems show varying degrees of π-localizations. In this manner, the practice of drawing a circle inside of each hexagonal ring in PAH systems

and in the fused ring region(s) in asphaltenes should be discouraged.

It has been concluded by NMR studies that the fused ring regions in asphaltenes are aromatic. However, if we follow the so defined "aromatic" and "antiaromatic" definitions based on the counting of π-electrons, many of the PAH systems and fused ring regions in asphaltenes would have to behave as antiaromatic compounds with low stability, and this is not the case. It has been reported[101] that π-density delocalization is not always stabilizing. This supports the idea of localization of the π-density in resonant sextets in certain parts of the PAH structures. In other words, some regions of the molecule behave more like benzene and others more like olefins.

On the other hand, if it is considered that there is a resonant sextet in each hexagonal ring in PAHs, the group symmetry associated with each molecule would be different if localized resonant sextets and localized double bonds are considered. Because of this, the Dias[48−53] periodic table is not designed to distinguish the different PAH structural isomers. In Dias' periodic table, it is considered that all of the structural isomers have the same d_s, C_Y, C_{PA3}, and C_{Int} structural factors and exactly the same number of resonant sextets (N_R), which is exactly the same as the number of fused rings (nFAR). If this were the case, the variation of up to 416 nm (1.7549 eV), Table 4, in the HOMO−LUMO gap for the same FAR series would not be observed.

Acree and co-workers[54] were not able to find relationships between point groups (or symmetry elements) and fluorescence probe character for several series of PAHs. They were unable to predict from structural considerations which polycyclic aromatic hydrocarbons will exhibit probe character. We consider that this is because the presence of localized resonant sextets was not taken into account in the assignment of the molecular symmetries, which in many cases is reduced.

As we have discussed in section 5, the highest HOMO−LUMO gap corresponds to the PAH with more resonant rings and zigzag structure. The lowest HOMO−LUMO gap corresponds to the completely linear structure with only one resonant ring. The consistent change in the HOMO−LUMO gap in each series is explained in terms of a consistent increase in the number of resonant rings in each isomer. As a consequence of the change in the number of resonant rings in each isomer of a FAR series, there is a change in the structural parameters C_Y, C_{PA3}, and C_{Int} that must take into account the number of resonant sextets. Therefore, the need to define new structural terms arises.

We have defined the structural terms C_{PAr3} and C_{IntAr}, which take into account the number of resonant sextets in the isomers in a FAR series. C_{PAr3} defines the number of peripheral aromatic carbons in localized resonant sextets having a connectivity of 3, eq 18.

$$C_{PAr3} = C_{PA3} - I_{even}, \quad I = 2, 4, 6, \ldots \quad \text{until} \quad C_{PAr3} = 4 \tag{18a}$$

or

$$C_{PAr3} = C_{IntAr} - C_Y = C_{Ar} - H_{Ar} - C_Y \tag{18b}$$

and

$$C_{PAr3} = C_{IntAr} \qquad \text{for cata-condensed systems} \tag{18c}$$

H_{Ar} represents the number of aromatic protonated carbons or total hydrogen atoms bonded to carbon atoms in localized resonant rings (i.e., in aromatic sextets), C_{Ar}, eq 19.

$$H_{Ar} = C_{Ar} - C_{PAr3} - C_Y \tag{19}$$

C_{IntAr} is the total internal bridging carbons in the FAR region only in localized resonant rings, eq 20. C_Y remains unchanged.

$$C_{IntAr} = C_Y + C_{PAr3} \tag{20}$$

For PAH in zigzag and full resonant structures (FRS), $C_{PAr3} = C_{PA3}$. Linear systems only have one resonant ring; thus, the value of C_{PAr3} is 2 or 4, depending on whether the resonant ring is located in one of the extreme hexagons or in an internal hexagon. The location of the resonant ring in the linear systems will be determined by the symmetry, the highest symmetry is preferred. For the case of an odd number of fused rings, it will be located at the central hexagon, as it has been reported for anthracene (Figure 9) and pentacene, **5b**.[92,93,95,102] It has been concluded that the π-electrons are more and more concentrated toward the end regions in higher linear PAHs.[93]

In the case of naphthalene (Figure 9), there is a conjugated aromatic bridgehead carbon right on the fusing region of the two hexagons.[93,95,103] Because of this situation, it has been concluded by calculation of NICS[47] that naphthalene has two resonant rings. However, the "aromatic stabilization" due to the presence of one resonant ring in benzene is 36 kcal mol^{-1},[71] while the experimental data reported for naphthalene is 61 kcal mol^{-1}.[104] If naphthalene had two resonant rings, it would be expected to observe an energy of stabilization of 72 kcal mol^{-1}. Many polycyclic aromatic hydrocarbons can be considered to be formed by fusion of naphthalene molecules such as tetracene (**4b**) and perylene (**5c**). In these cases, it is difficult to assign the aromatic sextet to a particular hexagon ring because there is a sharing of a double bond in the connection of the two hexagons of the "naphthalenic unit".

We found, as an observation, that in general the Y-carbons (C_Y), which represent the internal carbons in the FAR region having a connectivity of three, also provide information of the location of the resonant sextets in the peri-section in PAHs and consequently in asphaltenes. This is true only in the peri-section because the cata-branches do not have internal Y-carbons and $C_Y = 0$ as explained earlier in section 4.1.

We came up with a simple rule to draw the most likely localization of the resonant rings (sextets) in polycyclic aromatic hydrocarbon compounds and in the fused ring region in asphaltenes. We have called it the *Y-rule* because it involves the Y-carbons. The Y-rule is only used for the peri-section of the FAR region in asphaltenes and in PAHs. This rule allows us to determine the positions of the resonant sextets without having to calculate the electronic structure of the system and allows us to determine the maximum number of sextets in the FAR region.

The Y-rule is phrased as follows: The resonant sextets are located in the hexagons that contain the C_Y (Y-carbons). All of the C_Y carbons of the corresponding stoichiometry have to be included.

When there are more than one possibility to locate the sextets due to the arrangement of the internal Y-carbons, the possibility that provides the higher symmetry and the higher number of sextets will be the most probable. For the cata regions, the Y-rule does not apply. However, linear cata-condensed PAHs have only one resonant ring.

Our Y-rule is based on topological information of the PAH system, such as the number of π electrons (related to N_R), number of fused rings (nFAR), and on molecular connectivity (C_Y, C_{Int}, C_{PA3}, d_s) and quantities derived from such information (C_A, H_A, P_C). To the best of our knowledge, the Y-rule

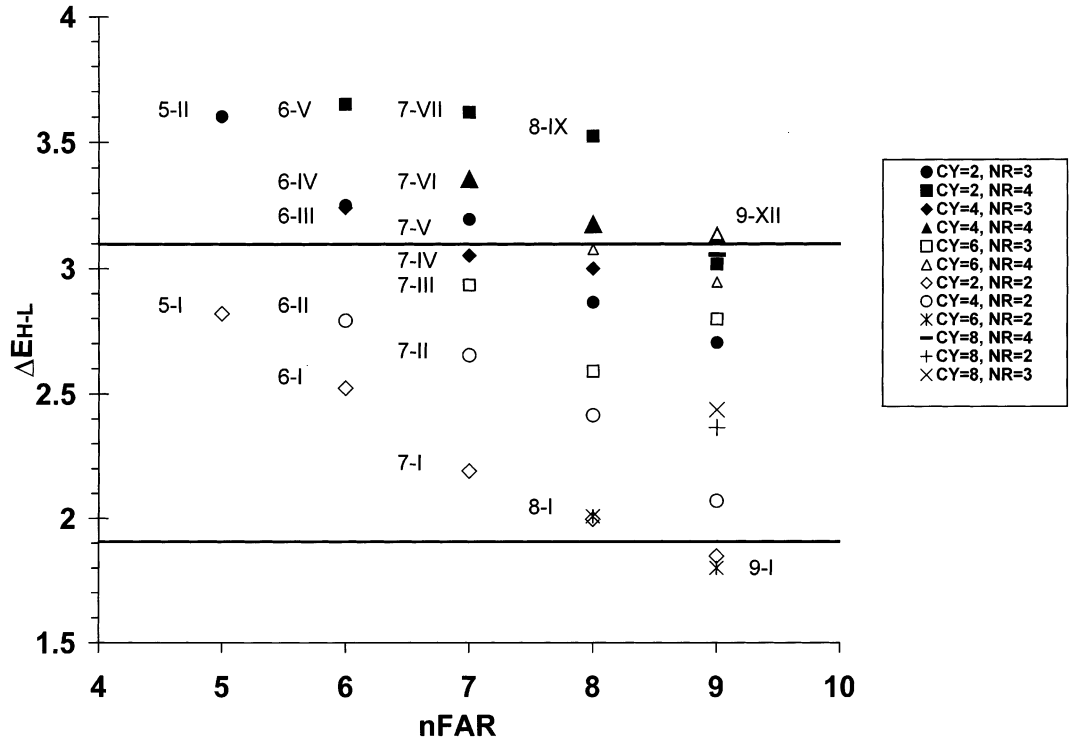

Figure 10. Diagram of ΔE_{H-L} versus the number of fused aromatic rings in benzenoid PAHs for several PAHs with different structural parameters: the number of internal Y-carbons (C_Y) and the number of resonant sextets (N_R). The two parallel thick lines delimit the experimental ΔE_{H-L} range observed for asphaltenes. The roman numbers are associated with the PAH structures given in Figure 11.

is the first of its kind. We could not find in the literature another rule similar to Y-rule. The topological characteristics of benzenoid PAHs are extrapolated to the aromatic fused regions in asphaltenes. Our observation has been supported by experimental NMR results. Iuliucci and co-workers[91] studied the ^{13}C chemical shift tensor of perylene and concluded that the distribution of the π-electrons is largely determined by the molecular connectivities.

The Y-rule is a rule to follow, a recipe to accommodate the total π-density distributed in sextets and double bonds in the σ-backbone not only in different isomers but also in any peri-PAH just by looking at the σ-backbone. The resulting π-distribution (in located sextets and located double bonds) obtained following the Y-rule explains the magnitudes of the HOMO−LUMO gap in structural isomers. Following the Y-rule, we are able to say which isomers are most likely to have a small HOMO−LUMO gap and which ones will have a big HOMO−LUMO gap.

For all of the peri-PAH systems studied here, 54 systems, we observe that the most likely location and consequently the total number of resonant sextets that explain the observed 0-0 fluorescence emission in benzenoid peri-PAH isomers and series involve all of the Y-carbons. The consequences of the Y-rule are to know how many sextets are present in the structures of benzenoid peri-PAH and their most likely location just by drawing the σ-backbone structure and visually locating the Y-carbons. On the other hand, the implications are that the fluorescence emission of the 0-0 band of PAH isomers and consequently of asphaltenes is better understood allowing this to determine the most likely structural and electronic characteristics of the PAH region in asphaltenes.

Much information can be obtained by only knowing the C or H content or both of a benzenoid PAH or a PAH region in asphaltenes. From Figure 1, the stoichiometry and number of fused rings can be determined as well as the percentage of compactness. The nearer the structure approaches to the upper limit, the higher the percentage of compactness is; also the percentage of compactness is given in Table 3. The number of Y-carbons can be calculated with eq 8. For example, $C_{28}H_{14}$ has $C_Y = 6$ with 8FAR, a percentage of compactness of 75%, and 28 π-electrons (the number of π-electrons is equal to the carbon content). To draw structural and consequently electronic isomers of this stoichiometry (some of them are already presented in Figure 7), the six Y-carbons have to be drawn first. In **8a**, **8c**, **8d**, and **8e** (Figure 7), the contour lines to draw six Y-carbons in space are depicted in bold. All of the contour lines are first drawn; then these lines are surrounded by hexagons to fulfill the property of the Y-carbons (internal carbons with connectivity of three). The missing hexagons to complete 8FAR are drawn, taking care to not exceed the H and C ratio. Finally the sextets are located following the Y-rule, and the distribution of the π-electrons is finished by placing the remaining π-electrons in double bonds, taking care of locating the double bonds without exceeding the valence of carbon atoms. By looking at the number of sextets drawn in each structure, we are able to say which structure will have a big HOMO−LUMO gap and which one will have the lowest HOMO−LUMO gap.

The Y-carbons not only are the internal carbons with a connectivity of three but also are the main core in the depiction of structures in PAH and in asphaltenes and are essential to depict the location of sextets following the Y-rule. The Y-rule is an empirical qualitative rule. However, its validity can be proven by studying the electronic structure of PAHs and also by comparing with results obtained from electric current calculations of PAHs. We are validating our Y-rule by the calculation of nuclear independent chemical shifts (NICS)[47] at the center of each hexagon in PAH compounds to determine the localization of the resonant rings.

There is a relation between the number of resonant sextets in the PAH structure and C_Y. For the case of asphaltenes, we have concluded that the fused ring region(s) are peri with cata-

TABLE 6: General Structural Data for the PAH Region in Asphaltenes

			upper structural limit						lower structural limit					
nFAR	formula	P_C (%)	C_Y	C_{PAr3}	N_R	ΔE_{H-L}[a]	structure	AS[c]	C_Y	C_{PAr3}	N_R	ΔE_{H-L}	structure	AS[c]
10FAR	$C_{40}H_{22}$	14	2	16	4									
				14	3									
9FAR	$C_{36}H_{20}$	16	2	12	4	3.0180	**9-IX**	Yes	2	4	2	1.8483	**9-II**	No
			2	10	3	2.7032	**9-VI**	Yes						
8FAR	$C_{32}H_{18}$	20	2	12	4	3.5240	**8-IX**	No	2	4	2	1.9961	**8-I**	Yes
			2	12	3	2.8646	**8-V**	Yes						
7FAR	$C_{28}H_{16}$	25	2	10	4	3.6188	**7-VII**	No	2	4	2	2.1912	**7-I**	Yes
			2	10	3	3.1961	**7-V**	No						
6FAR	$C_{24}H_{14}$	33	2	8	4	3.6504	**6-V**	No	2	4	2	2.5232	**6-I**	Yes
			2	6	3	3.2524	**6-IV**	No						
5FAR	$C_{20}H_{12}$	50	2	6	3	3.6020	**5-II**	No	2	4	2	2.8193	**5-I**	Yes
10FAR	$C_{38}H_{20}$	28	4	14	3, 4									
9FAR	$C_{34}H_{18}$	33	4	12	4	3.1333	**9-XI**	Yes	4	6	2	2.0697	**9-III**	Yes
8FAR	$C_{30}H_{16}$	45	4	10	4	3.1792	**8-VII**	Yes	4	4	2	2.4146	**8-III**	Yes
			4	8	3	3.0005	**8-VI**	Yes						
7FAR	$C_{26}H_{14}$	67	4	8	4	3.3576	**7-VI**	No	4	4	2	2.6537	**7-II**	Yes
			4	8	3	3.0527	**7-IV**	Yes						
6FAR	$C_{22}H_{12}$	82	4	6	3	3.2423	**6-III**	No	4	4	2	2.7916	**6-II**	Yes
10FAR	$C_{36}H_{18}$	49	6	12	4									
9FAR	$C_{32}H_{16}$	60	6	10	4	3.1336	**9-XII**	Yes	6	4	2	1.8008	**9-I**	No
			6	10	4	2.9457	**9-VIII**	Yes						
			6	8	3	2.7974	**9-VII**	Yes						
8FAR	$C_{28}H_{14}$	75	6	8	4	3.0772	**8-VII**	Yes	6	4	2	2.0080	**8-II**	Yes
			6	6	3	2.5899	**8-IV**	Yes						
7FAR	$C_{24}H_{12}$	100	6	6	3	2.9343	**7-III**	Yes						
10FAR	$C_{34}H_{16}$	66	8	10	4									
9FAR	$C_{30}H_{14}$	89	8	8	4	3.0557	**9-X**	Yes	8	4	3[b]	2.3650	**9-IV**	Yes
			8	6	3	2.4367	**9-V**	Yes						
10FAR	$C_{32}H_{14}$	100	10	8	4	2.8442	**10-I**	Yes						

[a] ΔE_{H-L} values were obtained using the force field optimized and ZINDO/S calculations. [b] It is not possible to get the $N_R = 2$ with $C_Y = 8$ combination. [c] AS = asphaltene structure. This column refers to the possible structure of the fused ring region in asphaltenes.

branches with 5−10 fused rings. In Figure 10, the HOMO−LUMO gap vs the number of fused rings for several PAH compounds with a percentage of compactness different from 0% and 100% are plotted. The two horizontal bars represent the experimental fluorescence emission of asphaltenes. The PAH systems have different number of sextets (N_R) in the structure and different number of internal Y-carbons (C_Y). The same information is presented in Table 6, and the structures associated with the roman numbers are drawn in Figure 11.

In general for each C_Y and N_R combination, there is a decrease in the HOMO−LUMO gap as the number of fused rings (nFAR) is increased (Figure 10). The systems with a high number of resonant sextets are near the upper experimental border of asphaltenes, and the systems with a low number of resonant sextets are in the lower experimental border of asphaltenes.

It can be derived from Figure 10 and Table 6 that in general the highest number of sextets in the PAH structure produces a HOMO−LUMO gap that does not fall into the experimental result for asphaltenes. The lowest number of resonant rings ($N_R = 2$) produces a HOMO−LUMO gap that is out of the experimental range for asphaltenes in the case of 9FAR and that is almost out of the asphaltene experimental range in the case of 8FAR. For 5FAR to 7FAR systems with $C_Y = 2$ or 4 and $N_R = 3$ or 4 combinations, the HOMO−LUMO gap is in general out of the experimental HOMO−LUMO gap of asphaltenes, and in the case of 9FAR, only the systems with four resonant rings are out (Figure 10).

The PAH compounds that are most likely to be good structural candidates of the aromatic fused ring region in asphaltenes are identified in Table 6 under the column AS (asphaltene structure). The HOMO−LUMO gaps of these polycyclic aromatic hydrocarbon compounds fall into the experimental 0-0 fluorescence emission region of asphaltenes and have a size (longest dimension) and molecular weight that agrees with the experimental data.

In general, we found that PAH systems with a percentage of condensation (P_C) between 75% and 100% can present the highest number of resonant sextets (N_R) in the structure calculated with eq 12 and fall into the asphaltene fluorescence emission experimental range. For PAH systems with a percentage of condensation $P_C < 75\%$, $N_R - 1$ is observed to fall into the experimental fluorescence range of asphaltenes, and for those stoichiometries that also are stoichiometries of full resonant structures (see Table 3), $N_R - 2$ is observed to fall into the experimental fluorescence range of asphaltenes.

Table 7 was obtained from analysis of Figure 10 and Table 6. In Table 7, the structural characteristics of the PAH systems that are most likely structural candidates of the fused ring region in asphaltenes from 5FAR to 10FAR, including also the number of allowed or most likely number of resonant sextets in asphaltenes, are presented. Table 7 is complemented with Table 6.

PAH systems that are not considered in Table 7 are not good structural candidates for asphaltenes. We hope that this table can help experimentalists and researchers in the area of asphaltenes to propose more realistic models of asphaltenes that match better with the experimental results of fluorescence, size (longest dimension), and weight.

The general idea that we pursue with the present research is to provide a general tool to propose most likely structural candidates for the fused aromatic ring region in asphaltenes. By NMR, the aromatic carbon and aromatic hydrogen content can be determined, as well as the number of substituted carbons in the aromatic fused region. Also, NMR can measure the number of internal Y-carbons. With this experimental information and the use of the formulas given in this paper, the number

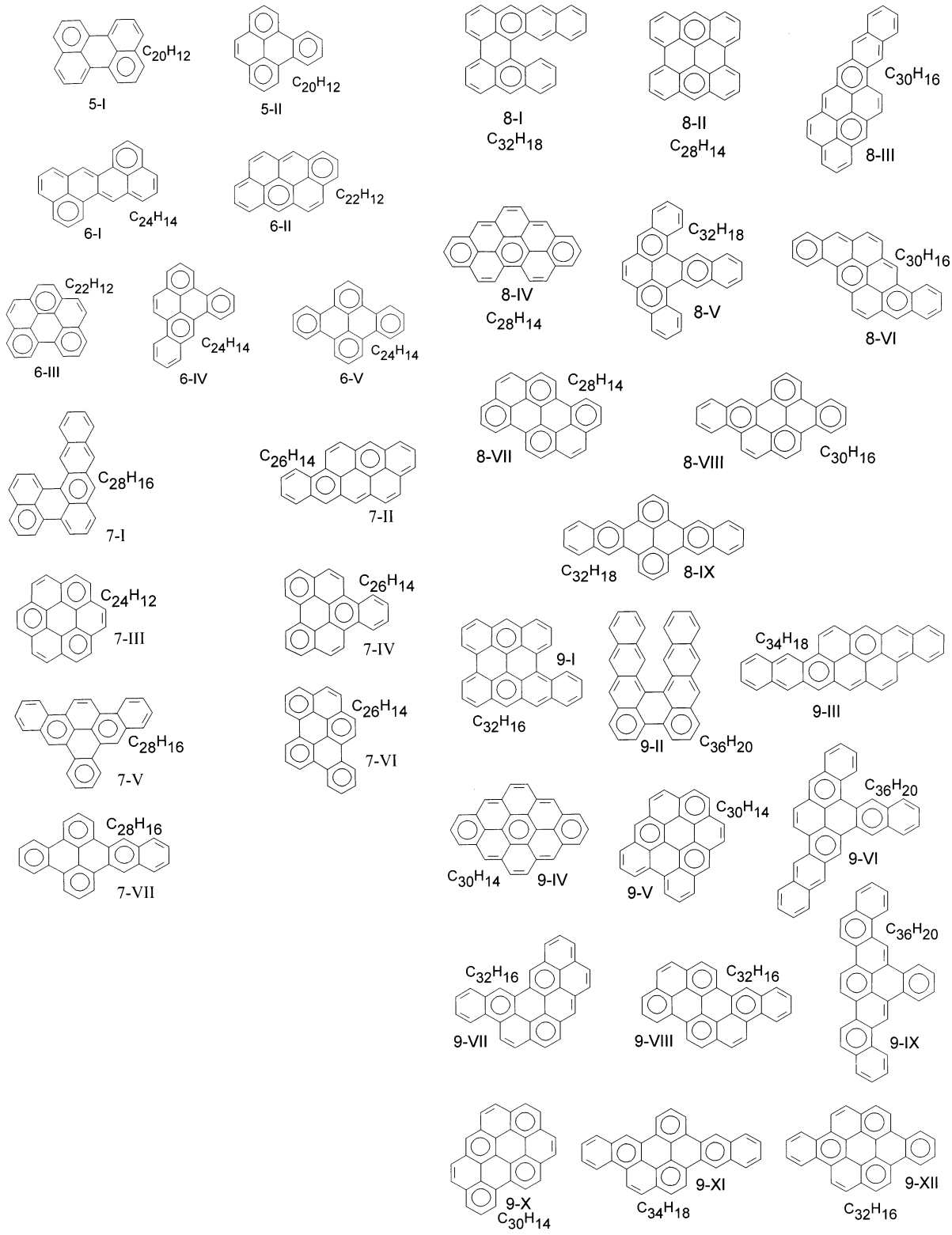

Figure 11. Structures of the PAH compounds that are considered in Table 6 and Figure 10.

of fused rings in the sample can be determined, as well as the number of possible resonant sextets and the percentage of compactness, and the most likely structural candidates can be determined from all of the structural data given in Table 7. The use of the Y-rule will allow locating the resonant rings to complete the structure. The obtained structural candidates can be tested to fit all of the other experimental information obtained for the samples, that is, molecular weight, size, fluorescence emission, etc.

The topological characteristics of benzenoid PAHs have previously been extrapolated to the aromatic ring region of asphaltenes,[105,106] but the effect of the presence of different number of resonant sextets in the PAH structures was not taken into account in the differentiation of possible structural isomers.

In Table 8, the HOMO−LUMO gap (ΔE_{H-L}) and associated λ for some asphaltene structures and their corresponding PAH's are presented. The structures of the systems mentioned in Table 8 are shown in Figure 12. The asphaltene structures in Figure

TABLE 7: Nonradical Benzenoid PAH Systems and Structural Parameters That Are Allowed as Structure of the Aromatic Region in Asphaltenes

nFAR	allowed stoichiometry	P_C (%)	allowed N_R in asphaltenes	d_s	C_Y	C_{PAr3}	C_{IntAr}
5FAR	$C_{20}H_{12}$	50	2	1	2	6	8
			2	1	2	4	6
6FAR	$C_{22}H_{12}$	82	3	0	4	6	10
			2	0	4	4	8
	$C_{24}H_{14}$	33	3, 2	2	2	8	10
			3, 2	2	2	6	8
			2	2	2	4	6
7FAR	$C_{24}H_{12}$	100	3	−1	6	6	12
	$C_{26}H_{14}$	65	3	1	4	8	12
			2	1	4	6	10
			2	1	4	4	8
	$C_{28}H_{16}$	25	3	3	2	10	12
			3, 4	3	2	8	10
			3, 4	3	2	6	8
			2	3	2	4	6
8FAR	$C_{28}H_{14}$	75	4	0	6	8	14
			3	0	6	6	12
			2	0	6	4	10
	$C_{30}H_{16}$	45	4	2	4	10	14
			3	2	4	8	12
			3, 2	2	4	6	10
			2	2	4	4	8
	$C_{32}H_{18}$	20	3	4	2	12	14
			4, 3	4	2	10	12
			3, 2	4	2	8	10
			2	4	2	6	8
			2	4	2	4	6
9FAR	$C_{30}H_{14}$	89	4	−1	8	8	16
			3	−1	8	6	14
			3	−1	8	4	12
	$C_{32}H_{16}$	60	4	1	6	10	16
			3	1	6	8	14
			3, 2	1	6	6	12
	$C_{34}H_{18}$	33	4	3	4	12	16
			3	3	4	10	14
			3	3	4	8	12
			3, 2	3	4	6	10
	$C_{36}H_{20}$	16	4	5	2	14	16
			4	5	2	12	14
			3	5	2	10	12
			3	5	2	8	10
			3	5	2	6	8
10FAR	$C_{32}H_{14}$	100	4	−2	10	8	10
	$C_{34}H_{16}$	66	4	0	8	10	18
			3	0	8	8	16
			3	0	8	6	14
	$C_{36}H_{18}$	49	4	2	6	12	18
			4, 3	2	6	10	16
			3	2	6	8	14
			3	2	6	6	12
	$C_{38}H_{20}$	28	4, 3	4	4	14	18
			4, 3	4	4	12	16
	$C_{40}H_{22}$	14	4, 3	6	2	16	18
			4, 3	6	2	14	14

12 have been reported in the literature. The calculated sizes of the reported asphaltene structures (Table 8) fall into the experimental range of 10−20 Å.[13]

By comparing the calculated HOMO−LUMO gap for the different asphaltene structures with their corresponding polycyclic aromatic hydrocarbon cores, we found that the effect of the presence of the alkyl chains and the heteroatoms in the asphaltene structures on the HOMO−LUMO gap is almost negligible (Table 8). The HOMO−LUMO gap of the corresponding PAH is very similar to the one of the whole asphaltene. The fused ring region(s) in asphaltenes contains heteroatoms (N, O, S). A red shift of up to 37 nm in the wavelength is observed in the HOMO−LUMO gap of the asphaltene structures

TABLE 8: Calculated Size, HOMO−LUMO Gap (ΔE_{H-L}), and Associated λ for Reported Asphaltenes Structures and Their Corresponding PAHs

system	size (Å)	ΔE_{H-L} (eV)	associated λ (nm)
cata-asphaltene1[a]	14.86	3.5536	348.72
4a	11.43	3.8632	320.78
cata-asphaltene2[a]	17.85	3.2991	375.63
5a	13.51	3.6423	340.23
asphaltene1[b]	22.70	2.8884	429.03
6f	13.51	3.0139	411.17
asphaltene2[b]	26.69	2.2883	543.01
6g	11.43	2.4027	515.76
asphaltene3[b]	24.12	2.8771	430.72
5c	11.41	3.1500	393.40
PAC	14.95	2.9993	413.17

[a] Reference 107. [b] Reference 14.

compared with the wavelength of the corresponding PAH (Table 8) because of the presence of the heteroatoms in the asphaltene structures.[61,62]

We have concluded in this work that a polycyclic aromatic hydrocarbon core with a percentage of condensation of 0%, that is, in linear or zigzag arrangements, is not likely to be present in the asphaltene structures. Thus, it is observed that the calculated HOMO−LUMO gap of the **cata-asphaltene1** and **cata-asphaltene2** structures (Table 8) does not fall into the experimental fluorescence range of 400−650 nm[13] reported for asphaltenes. The polycyclic aromatic hydrocarbon core of these structures corresponds to a zigzag PAH with four fused aromatic rings (4FAR, **4a**) for **cata-asphaltene1** and a zigzag PAH with five fused aromatic rings (5FAR, **5a**) for **cata-asphaltene2** (see Figure 12). The HOMO−LUMO gap of **4a** and **5a** does not fall into the experimental fluorescence range of asphaltenes either. We consider that the proposed structures of these asphaltenes need to be checked and reconsidered. The polycyclic aromatic hydrocarbon cores in these structures are not good candidates for asphaltenes.

It has been observed[62] that the Urbach phenomenology, in which the absorption coefficient depends exponentially on the photon energy, describes the absorption spectral profile of crude oils and asphaltenes when absorption is dominated by HOMO−LUMO transitions. The absorption spectra profile, therefore, provides a measure of the population distribution of molecules.[62] For heavy crude oils and asphaltenes, the absorption at short wavelengths is smaller than that predicted from an extrapolation of the Urbach tail. Thus, the relative population of blue-absorbing chromophores (small chromophores) is less compared with the population of red-absorbing chromophores (big chromophores).[62] So, **4a**, which is a small chromophore, cannot be a good candidate for the aromatic fused ring region in asphaltenes.

The polyaromatic core in **asphaltene1** is related to dibenzo[*a*,*i*]pyrene, **6f** (Figure 12). The calculated HOMO−LUMO gap of **asphaltene1** and **6f** falls into the experimental fluorescence range of asphaltenes. We consider that the proposed structure and polycyclic aromatic hydrocarbon core of **asphaltene1** is most likely to be realistic.

The structure **6f** presents as structural parameters the following: six fused aromatic rings (6FAR), a stoichiometry of $C_{24}H_{14}$, 33% of condensation, three resonant sextets ($N_R = 3$), a net number of disconnections among the internal edges of two ($d_s = 2$), two internal aromatic carbons having a connectivity of three ($C_Y = 2$), six peripheral aromatic carbons in localized resonant sextets having a connectivity of three ($C_{PAr3} = 6$), and eight total internal bridging carbons in localized resonant rings

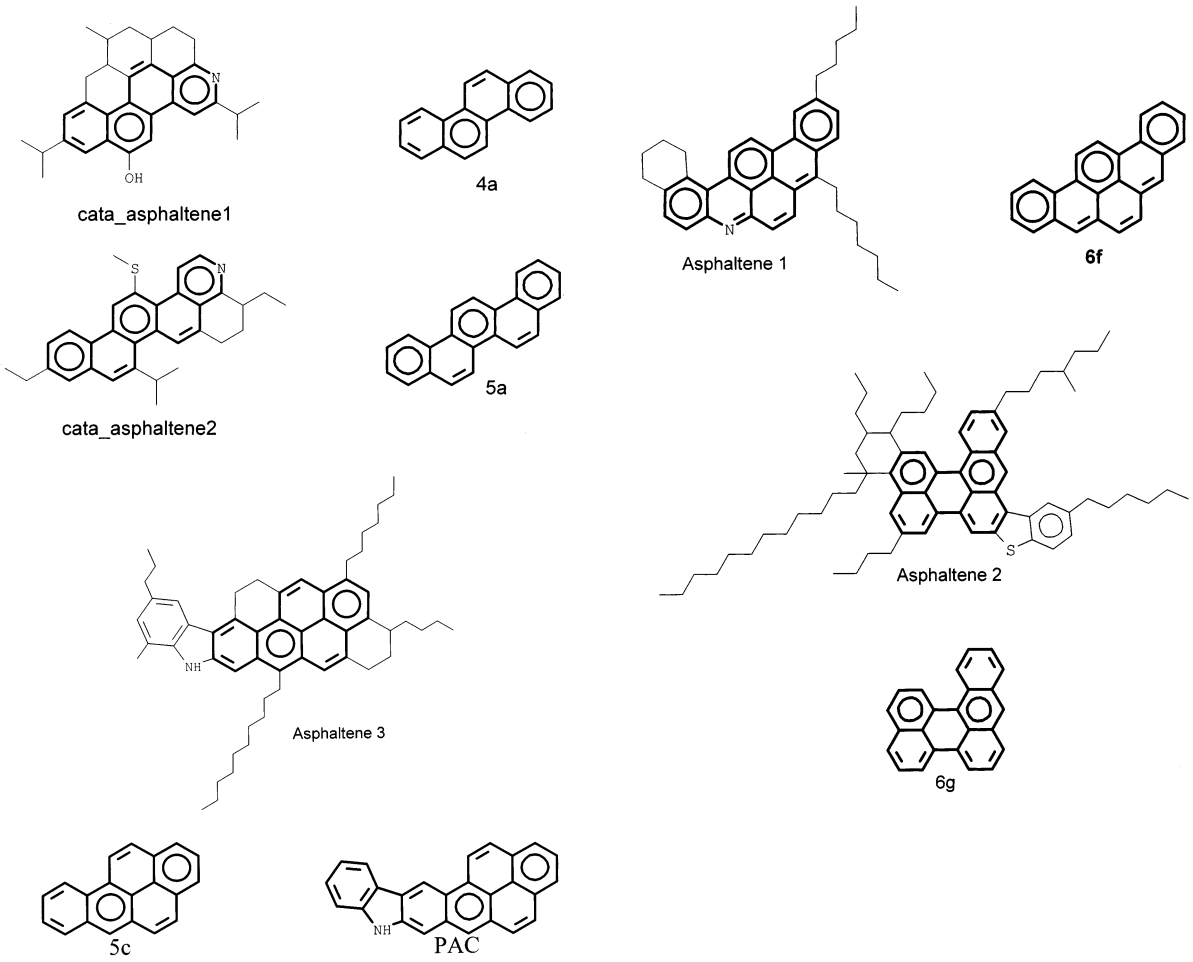

Figure 12. Reported asphaltene structures and their associated PAH core.

($C_{IntAr} = 8$). All of these structural parameters are listed in Table 7, which presents the structural parameters of nonradical benzenoid polyaromatic hydrocarbons allowed as structures of the aromatic fused region in asphaltenes.

The polyaromatic core in **asphaltene2** is related to benzo[*a*]perylene, **6g** (Figure 12). The calculated HOMO−LUMO gap of **asphaltene2** and **6g** falls into the experimental fluorescence range of asphaltenes. The proposed structure and polycyclic aromatic hydrocarbon core of **asphaltene2** is also most likely to be realistic.

The structure **6g** presents the same structural parameters as **6f** with the difference that the number of resonant sextets in **6g** is two ($N_R = 2$). All of the structural parameters of **6g** are also included in Table 7. Isomers **6g** and **6f** are structural isomers. Isomer **6f** and the polyaromatic ring region in **asphaltene1** tend to be more planar than **6g** and the polyaromatic ring region in **asphaltene2** because of the presence of a cove region in **6g** (Figure 4). The hydrogen atoms in the cove region are too closed, which breaks the planarity in this region.

The structure of **asphalthene2** presents sulfur in its aromatic region in the thiophenic form, which is the dominant form of sulfur in asphaltenes.[108] The thiophenic sulfur is not considered in the structure of the associated polycyclic aromatic hydrocarbon core (**6g**); however, the effect of the presence of the thiophenic sulfur on the HOMO−LUMO gap of the whole **asphaltene2** compared with the HOMO−LUMO gap of **6g** is almost negligible (Table 8). That is not the case with the presence of the pyrrolic nitrogen in the structure of **asphaltene3**. Pyrrolic and pyridinic nitrogen are the most prevalent forms of nitrogen in asphaltenes. Pyrrolic nitrogen is more abundant than the pyridinic form.[109] The HOMO−LUMO gap of the structure of **asphaltene3** falls into the range of the experimental fluorescence emission of asphaltenes, and the associated benzenoid polyaromatic hydrocarbon, **5c**, presents a HOMO−LUMO gap that is close to that of asphaltenes. The difference in the HOMO−LUMO gap of **asphaltene3** and **5c** is 37.32 nm. We could say that this difference is not too big and that it is due to the presence of the pyrrolic nitrogen; however, pyrrolic nitrogen seems to produce a greater red shift (37.32 nm) than the piridinic nitrogen (17.86 nm) observed in the case of **asphaltene1** and **6f**. On the other hand, the HOMO−LUMO gap of the whole polyaromatic compound, PAC, included in **asphaltene3** (Figure 12) presents a smaller red shift compared with the HOMO−LUMO gap of the whole **asphaltene3** structure (17.55 nm), Table 8. We consider that **asphaltene3** is a good structural candidate of an asphaltene. The structural characteristics of the aromatic region of **5c** are also included in Table 7, which makes it a good polycyclic aromatic hydrocarbon candidate for the aromatic region in asphaltenes.

8. Conclusions

To address a currently existing controversy regarding the number of fused aromatic rings in the fused ring region core in petroleum asphaltenes, we have studied the HOMO−LUMO gap as an index of molecular size and structure for polycyclic aromatic hydrocarbons (PAHs) and extended the findings to asphaltenes. Structural relationships between the HOMO−LUMO gap in free nonradical benzenoid polyaromatic hydrocarbons (PAHs) and the distribution of the fused rings in these

structures were obtained. We found that the magnitude of the HOMO−LUMO gap in PAH is closely related to the number of fused aromatic rings (nFAR), to the spatial arrangement of the fused rings, to the percentage of compactness (P_C) of the structure, and to the number and location of resonant sextets (N_R) in the structure.

The consistent change in the HOMO−LUMO gap in each PAH series with the same number of fused aromatic rings, which increases going from the linear arrangement to the most compact arrangement, is explained in terms of a consistent increase in the number of localized resonant sextets going from the linear arrangement with a degree of compactness of $P_C = 0\%$ to the circular ($P_C = 100\%$) or most compact (highest P_C) arrangements. The polycyclic aromatic hydrocarbons with zigzag arrangement ($P_C = 0\%$) together with the polycyclic aromatic hydrocarbons with a full resonant structure (FRS) have the largest HOMO−LUMO gap and the highest number of resonant sextets in their structure. The polycyclic aromatic hydrocarbons with linear arrangement present the lowest HOMO−LUMO gap and only one resonant sextet in the structure.

The magnitude of the HOMO−LUMO gap of polycyclic aromatic hydrocarbons in arrangements different from linear, zigzag, and FRS, that is, peri-type with cata-branches, fall inside the linear−zigzag HOMO−LUMO gap region. From 4FAR to 6FAR, there is an average change in the HOMO−LUMO gap between the zigzag and the linear structures of 1.4586 eV, while from 6FAR to 14FAR, there is an average change of 1.7420 eV.

The full resonant structures (FRS) have an integer number of resonant sextets and no double bonds. However, all of the other PAH systems that are not FRS, reach a maximum number of resonant sextets with accompanying localized double bonds in their structures. In other words, some regions of the molecule behave more like benzene and others more like olefins in agreement with the findings of previous investigations.

We consider that the practice of drawing a circle inside of each hexagonal ring in PAH systems and in the fused ring region(s) in asphaltenes should be discouraged. Only in the case of FRS the circle notation to represent the aromatic sextets could be used to depict delocalization because all of the carbon atoms—and all of the available π-density—are participating in resonant sextets.

As a consequence of the change in the number of resonant rings in each PAH isomer of a fused aromatic ring (FAR) series, there is a change in the structural parameters that must take into account the number of resonant sextets. Therefore, the need to define new structural terms arises. We have defined structural terms that take into account the number of resonant sextets in the isomers in a FAR series and found relationships between the number of internal carbons with a connectivity of three that participate in resonant sextets, the number of sextets in the structure, and the magnitude of the HOMO−LUMO gap. In general, the increment of one more resonant ring between structural isomers opens up the HOMO−LUMO gap by approximately 0.4−0.5 eV. The opening of the HOMO−LUMO gap could be less if holes, coves, and fjords are present in the structure.

In this paper, we present a new qualitative rule that we have called the *Y-rule* that helps to determine the number of resonant sextets and to draw their most likely localization in homologous series of polycyclic aromatic hydrocarbon compounds and in the fused ring region in asphaltenes. The Y-rule only applies for the peri-section of the fused ring region in asphaltenes and in PAH with fused six-member rings.

These results are extrapolated to the fused aromatic ring region in asphaltenes. The experimental HOMO−LUMO gap range of asphaltenes obtained from fluorescence emission data was compared with the calculated HOMO−LUMO gap of free PAHs. By comparing the calculated HOMO−LUMO gap for the different asphaltene structures with their corresponding polycyclic aromatic hydrocarbon cores, we found that the effect of the presence of the alkyl chains and the heteroatoms in the asphaltene structures on the HOMO−LUMO gap is almost negligible. We conclude that the asphaltene experimental fluorescence emission range does not necessarily correspond to different chromophores with different number of fused aromatic rings (FAR) but to different isomers with the same number of FAR but with different number of resonant sextets in the structure.

We conclude that it is possible to have a small PAH chromophore and a big PAH chromophore, in terms of the number of fused rings, with a 0-0 fluorescence emission band in the same region. Thus, the statement that short-wavelength excitation produces excitation of small chromophores and that correspondingly long-wave excitation produces excitation of large chromophores is only valid if by small or big chromophore reference to the size (longest dimension in Å) not to the number of fused rings is made.

We conclude that there are 5−10 fused aromatic rings in each fused ring region in asphaltenes. The zigzag and linear arrangements, which have a percentage of compactness of 0%, and the full resonant structures (despite the degree of condensation) cannot be candidates for the fused region in asphaltenes. The circular structures with a compactness of 100%, coronene (7FAR, **7c**) and ovalene (10FAR, **10a**), might be structural candidates of the fused ring region in asphaltenes, any other circular structure is not possible.

Polycyclic aromatic hydrocarbon cores with a percentage of condensation different from 0% and 100% with structural combinations of $C_Y = 2$, 4, 6, and 8 internal carbons with a connectivity of three (Y-carbons) that form part of resonant sextets, $C_{ArP3} = 14$, 12, 10, 8, 6, and 4 external carbons with a connectivity of three that form part of resonant sextets, and $N_R = 4$, 3, and 2 total number of resonant sextets in the structure are good structural candidates for the fused ring regions in asphaltenes. The structural combination $C_{ArP3} = 4$ and $N_R = 2$ is not possible for 9FAR and 10FAR. Polycyclic aromatic hydrocarbon cores that do not present these combinations of structural parameters have a HOMO−LUMO gap that is not inside the experimental fluorescence range of asphaltenes and most likely are not good candidates of the ring region in asphaltenes.

Acknowledgment. Y.R.-M. gratefully acknowledges Silicon Graphics Inc. for allowing us to carry most of the calculations on their supercomputer called Typhoon (a 512-processor Origin 2000). Thanks are due to Dr. Oliver Mullins for fruitful and motivating discussions. The assistance of Dr. Gerardo Cisneros for his help with the installation of Gaussian 98 and benchmarking of the runs and Ms. Mireya Villanueva for her help with system administration is gratefully acknowledged.

References and Notes

(1) *Bitumens, Asphalts, and Tar Sands*; Chilingarian, G. V., Yen, T. F., Eds.; Elsevier: New York, 1978.

(2) Speight, J. G. *The Chemistry and Technology of Petroleum*; Marcel Dekker: New York, 1980; pp 189−252.

(3) Tissot, B. P.; Welte, D. H. *Petroleum Formation and Occurrence*, 2nd ed.; Springer-Verlag: Berlin, 1984.

(4) *Chemistry of Asphaltenes*; Bunger, J. W., Li, N. C., Eds.; American Chemical Society: Washington, 1984.

(5) *Asphaltenes, Fundamentals and Applications*; Sheu, E. Y., Mullins, O. C., Eds.; Plenum Press: New York, 1995.
(6) *Structures and Dynamics of Asphaltenes*; Mullins, O. C., Sheu, E. Y., Eds.; Plenum Press: New York, 1998.
(7) Speight, J. G. *Fuel* **1970**, *49*, 76.
(8) Yen, T. F. *Energy Sources* **1974**, *1*, 447.
(9) Suzuki, T.; Itoth, M.; Takegani, Y.; Watanabe, Y. *Fuel* **1982**, *61*, 402.
(10) Miller, J. T.; Fisher, R. B.; Thiyagarajan, P.; Winans, R. E.; Hunt, J. E. *Energy Fuels* **1998**, *12*, 1290.
(11) Artok, A.; Su, Y.; Hirose, Y.; Hosokawa, M.; Murata, S.; Nomura, M. *Energy Fuels* **1999**, *13*, 287.
(12) Wiehe, I. A. *Energy Fuels* **1994**, *8*, 536.
(13) Groenzin, H.; Mullins, O. *J. Phys. Chem. A* **1999**, *103*, 11237 and references therein.
(14) Groenzin, H.; Mullins, O. *Energy Fuels* **2000**, *14*, 677.
(15) The molecular weight of asphaltenes is reported in amu; 1 amu is equivalent to 1 g/mol.
(16) Anderson, S. I.; Speight, J. G. *Fuel* **1993**, *72*, 1343.
(17) Boduszynski, M. M. In *Asphaltenes, Fundamentals and Applications*; Sheu, E. Y., Mullins, O. C., Eds.; Plenum Press: New York, 1995; Chapter 7.
(18) Boduszynski, M. M. *Energy Fuels* **1988**, *2*, 597.
(19) Strausz, O. P.; Mojelsky, T. W.; Lown, E. M. *Fuel* **1992**, *71*, 1355.
(20) Zajac, G. W.; Sethi, N. K.; Joseph, J. T. *Scanning Microsc.* **1994**, *8*, 463.
(21) Aihara, J. *J. Phys. Chem. A* **1999**, *103*, 7487.
(22) Aihara, J. *Theor. Chem. Acc.* **1999**, *102*, 134.
(23) Aihara, J. *Phys. Chem. Chem. Phys.* **1999**, *1*, 227.
(24) Parr, R. G.; Zhou, Z. *Acc. Chem. Res*. **1993**, *26*, 256.
(25) Liu, X.; Schmalz, T. G.; Klien, D. *J. Chem. Phys. Lett*. **1992**, *18*, 550.
(26) Haddon, R. C.; Fukunaga, T. *Tetrahedron Lett.* **1988**, *29*, 4843.
(27) Pearson, R. G. *Hard and Soft Acids and Bases*; Dowden, Hutchinson and Ross: Stroudsburg, PA, 1973.
(28) Manolopoulos, D. E.; May, J. C.; Down, S. E. *Chem. Phys. Lett.* **1991**, *181*, 105.
(29) Clar, E. *Polycyclic Hydrocarbons*; Academic: London, 1964.
(30) Clar, E. *The Aromatic Sextet*; Wiley: London, 1972.
(31) Hess, B. A., Jr.; Scaad, L. J. *J. Am. Chem. Soc.* **1971**, *93*, 2413.
(32) Zhou, Z.; Parr, R. G.; Garst, J. F. *Tetrahedron Lett.* **1988**, *29*, 4843.
(33) Zhou, Z.; Parr, R. G. *J. Am. Chem. Soc.* **1989**, *111*, 7371.
(34) Havenith, R. W. A.; van Lenthe, J. H.; Dijkstra, F.; Jenneskens, L. W. *J. Phys. Chem. A* **2001**, *105*, 3838.
(35) Minkin, V. I.; Glukhovtsev, M. N.; Sinkin, B. Y. *Aromaticity and Antiaromaticity. Electronic and Structural Aspects*; J. Wiley: New York, 1994.
(36) Krygowki, T. M.; Cyranski, M. K. *Chem. Rev.* **2001**, *101*, 1385.
(37) Gomes, J. A. N. F.; Mallion, R. B. *Chem. Rev.* **2001**, *101*, 1349.
(38) De Proft, F.; Geerlings, P. *Chem. Rev.* **2001**, *101*, 1451.
(39) Mitchell, R. H. *Chem. Rev.* **2001**, *101*, 1301.
(40) Garrat, P. J. *Aromaticity*; John Wiley and Sons: New York, 1986; Chapter 9.
(41) Platt, J. R. *J. Chem. Phys*. **1954**, *22*, 144.
(42) Volpin, M. E. *Russ. Chem. Rev.* **1960**, *29*, 129.
(43) Craig, D. P. *J. Chem. Soc*. **1951**, 3175.
(44) Hosoya, H.; Hosi, K.; Gutman, I. *Theor. Chim. Acta* **1975**, *38*, 37.
(45) Aihara, J. *J. Org. Chem*. **1976**, *41*, 2488.
(46) Aihara, J. *J. Am. Chem. Soc*. **1977**, *99*, 2048.
(47) Schleyer, P. v. R.; Maerker, C.; Dransfeld, A.; Jiao, H.; Hommes N. J. R. v. E. *J. Am. Chem. Soc*. **1996**, *118*, 6317.
(48) Dias, J. R. *Polycyclic Aromat. Compd.* **1994**, *4*, 87.
(49) Dias, J. R. *J. Mol. Struct. (THEOCHEM)* **1993**, *284*, 11.
(50) Dias, J. R. *J. Mol. Struct. (THEOCHEM)* **1991**, *230*, 155.
(51) Dias, J. R. *Theor. Chim. Acta* **1990**, *77*, 143.
(52) Dias, J. R. *Polycyclic Aromat. Compd.* **1999**, *14*−*15*, 63.
(53) Dias, J. R. *Acc. Chem. Res.* **1985**, *18*, 241.
(54) Acree, W. E., Jr.; Tucker, S. A. *Polycyclic Aromat. Compd.* **1991**, *2*, 75.
(55) Molecular Simulation Incorporated. *Cerius*^{2} *Modeling Environment*, release 4.0; Molecular Simulations Incorporated: San Diego, CA, 1999.
(56) Sun, H.; Ren, P.; Fried, J. R. *Comput. Theor. Polym. Sci.* **1998**, *8*, 229.
(57) Sun, H. *J. Phys. Chem. B* **1998**, *102*, 7338.
(58) Ruiz-Morales, Y., manuscript in preparation.
(59) Zerner, M. C.; Correa de Mello, P.; Hehenberger, M. *Int. J. Quantum Chem.* **1982**, *21*, 251.
(60) Frisch, M. J.; Trucks, G. W.; Schlegel, H. B.; Scuseria, G. E.; Robb, M. A.; Cheeseman, J. R.; Zakrzewski, V. G.; Montgomery, J. A., Jr.; Stratmann, R. E.; Burant, J. C.; Dapprich, S.; Millam, J. M.; Daniels, A. D.; Kudin, K. N.; Strain, M. C.; Farkas, O.; Tomasi, J.; Barone, V.; Cossi, M.; Cammi, R.; Mennucci, B.; Pomelli, C.; Adamo, C.; Clifford, S.; Ochterski, J.; Petersson, G. A.; Ayala, P. Y.; Cui, Q.; Morokuma, K.; Malick, D. K.; Rabuck, A. D.; Raghavachari, K.; Foresman, J. B.; Cioslowski, J.; Ortiz, J. V.; Stefanov, B. B.; Liu, G.; Liashenko, A.; Piskorz, P.; Komaromi, I.; Gomperts, R.; Martin, R. L.; Fox, D. J.; Keith, T.; Al-Laham, M. A.; Peng, C. Y.; Nanayakkara, A.; Gonzalez, C.; Challacombe, M.; Gill, P. M. W.; Johnson, B. G.; Chen, W.; Wong, M. W.; Andres, J. L.; Head-Gordon, M.; Replogle, E. S.; Pople, J. A. *Gaussian 98*, revision A.7; Gaussian, Inc.: Pittsburgh, PA, 1998.
(61) Berlman, L. B. *Handbook of Fluorescence Spectra of Aromatic Compounds*; Academic Press: New York, 1971.
(62) Mullins, O. C. In *Asphaltenes, Fundamentals and Applications*; Sheu, E. Y., Mullins, O. C., Eds.; Plenum Press: New York, 1995; Chapter 2.
(63) Scotti, R.; Montanari, L. In *Asphaltenes, Fundamentals and Applications*; Sheu, E. Y., Mullins, O. C., Eds.; Plenum Press: New York, 1995; Chapter 3.
(64) (a) Siegmann, K.; Hepp, H.; Sattler, K. *Combust. Sci. Technol*. **1995**, *109*, 165. (b) Siegmann, K.; Sattler, K. *J. Chem. Phys.* **2000**, *112*, 698.
(65) Hess, B. A., Jr.; Schaad, L. J. *J. Org. Chem.* **1971**, *36*, 3418.
(66) Herndon, W. C. *Tetrahedron* **1982**, *38*, 1389.
(67) Stein, S. E. *Acc. Chem. Res.* **1991**, *24*, 350.
(68) Klimkans, A.; Larsson, S. *Chem. Phys.* **1994**, *189*, 25.
(69) Yoshizawa, K.; Okahara, K.; Sato, T.; Tanaka, K.; Yamabe, T. *Carbon* **1994**, *32*, 1517.
(70) Cyvin, S. J.; Brunvoll, J.; Cyvin, B. N. *Polycyclic Aromat. Compd.* **1997**, *12*, 201.
(71) Schleyer, P. v. R.; Jiao, H. *Pure Appl. Chem.* **1996**, *68*, 209.
(72) Dias, J. R. *J. Chem. Inf. Comput. Chem.* **1991**, *31*, 89.
(73) (a) Dias, J. R. *Tetrahedron* **1993**, *49*, 9207. (b) Dias, J. R. *Chem. Phys. Lett*. **1993**, *204*, 486.
(74) (a) Dias, J. R. *Handbook of Polycyclic Hydrocarbons, Part A*; Elsevier: Amsterdam, 1987; pp 86−87. (b) Dias, J. R. *Handbook of Polycyclic Hydrocarbons, Part B*; Elsevier: Amsterdam, 1987; p 367.
(75) *Spectral Atlas of Polycyclic Aromatic Compounds*; Karcher, W., Fordham, R. J., Dubois, J., Glaude, P. G. M., Ligthart, J. A. M., Eds.; Reidel: Dordrecht, Netherlands, 1990.
(76) *Ultraviolet Spectra*; Sadtler Research Laboratories Inc.: Philadelphia, PA, 1975.
(77) McKay, J. F.; Latham, D. R. *Anal. Chem.* **1972**, *44*, 2132.
(78) Nakashima, K.; Yashuda, S.; Ozaki, Y.; Noda, I. *J. Phys. Chem. A* **2000**, *104*, 9113.
(79) Heinecke, E.; Hartmann, D.; Müller, R.; Hese, A. *J. Chem. Phys.* **1998**, *109*, 906.
(80) Halasinski, T. M.; Hudgins, D. M.; Salama, F.; Allamandola, L. J. *J. Phys. Chem. A* **2000**, *104*, 7484.
(81) Canuto, S.; Zerner, M. C.; Diercksen, G. H. F. *Astrophys. J.* **1991**, *377*, 150.
(82) Waris, R.; Street, K. W., Jr.; Acree, W. E., Jr.; Fetzer, J. C. *Appl. Spectrosc*. **1989**, *43*, 845.
(83) Trickey, S. B.; Diercksen, G. H. F.; Müller-Plathe, F. *UV Atlas of Organic Compounds*; Plenum: New York, 1967.
(84) Aihara, J.; Yamabe, T.; Hosoya, H. *Synth. Met.* **1994**, *64*, 309.
(85) Yoshizawa, K.; Yahara, K.; Tanaka, K.; Yamabe, T. *J. Phys. Chem. B* **1998**, *102*, 498 and references therein.
(86) Seki, H.; Kumata, F. *Energy Fuels*, **2000**, *14*, 980.
(87) Tyutyulkov, N.; Madjarova, G.; Diets, F.; Müllen, K. *J. Phys. Chem. B* **1998**, *102*, 10183 and references therein.
(88) Dewar, M. J. S. *The Molecular Orbital Theory of Organic Chemistry*; McGraw-Hill: New York, 1969.
(89) Hosoya, H.; Kumazaki, H.; Chida, K.; Ohuchi, M.; Gao, Y.-D. *Pure Appl. Chem.* **1990**, *62*, 445.
(90) Tanaka, K.; Yamashita, S.; Yamabe, H.; Yamabe, T. *Synth. Met.* **1987**, *17*, 143.
(91) Iuliucci, R. J.; Phung, C. G.; Facelli, J. C.; Grant, D. M. *J. Am. Chem. Soc.* **1996**, *118*, 4880.
(92) Ligabue, A.; Pincelli, U.; Lazzereti, P.; Zanasi, R. *J. Am. Chem. Soc.* **1999**, *121*, 5513.
(93) Suresh, C. H.; Gadre, S. R. *J. Org. Chem.* **1999**, *64*, 2505.
(94) Iuliucci, R. J.; Phung, C. G.; Facelli, J. C.; Grant, D. M. *J. Am. Chem. Soc.* **1998**, *120*, 9305.
(95) Lazzeretti, P. *Prog. Nucl. Magn. Reson. Spectrosc.* **2000**, *36*, 1.
(96) Lazzeretti, P.; Magagoli, M.; Zanasi, R. *J. Mol. Struct. (THEOCHEM)* **1991**, *234*, 127.
(97) Lindon, J.; Dailey, B. P. *Mol. Phys.* **1970**, *19*, 285.
(98) Khetrapal, C. L.; Kunwar, A. C. *Adv. Magn. Reson.* **1970**, *9*, 301.
(99) Jameson, A. K.; Jameson, C. J. *Chem. Phys. Lett*. **1987**, *134*, 461.
(100) Ruiz-Morales, Y.; Schreckenbach, G.; Ziegler, T. *Organometallics* **1996**, *15*, 3920.
(101) Yu, Z.-H.; Xuan, Z.-Q.; Wang, T.-X.; Yu, H.-M. *J. Phys. Chem. A* **2000**, *104*, 1736.
(102) Aihara, J. *J. Chem. Soc., Perkin Trans*. **1996**, *2*, 2185.

(103) Zanasi, R.; Lazzeretti, P. *Mol. Phys*. **1997**, *92*, 609.
(104) Wheland, G. W. *Resonance in Organic Chemistry*; Wiley: New York, 1955.
(105) Masuda, K.; Okuma, O.; Nishizawa, T.; Kanaji, M.; Matsumura, T. *Fuel* **1996**, *75*, 295.
(106) Hamaguchi, H.; Nishizawa, T. *Fuel* **1992**, *71*, 798.
(107) Sato, S.; Takanohashi, T.; Tanaka, R. *Prepr. Symp.−Am. Chem. Soc., Div. Fuel Chem.* **2001**, *46*, 353−354.
(108) Waldo, G. S.; Mullins, O. C.; Penner-Hahn, J. E.; Cramer, S. P. *Fuel* **1992**, *71*, 53.
(109) Mitra-Kirtley, S.; Mullins, O. C.; van Elp, J.; George, S. J.; Chen, J.; Cramer, S. P. *J. Am. Chem. Soc*. **1993**, *115*, 252.